Analytical and Bioanalytical Chemistry (2024) 416:3923–3944
https://doi.org/10.1007/s00216-024-05303-y

CRITICAL REVIEW

From synthesis to applications of biomolecule-protected luminescent gold nanoclusters

Jiafeng Qiu[1,2] · Faisal Ahmad[1,2] · Jianxin Ma[1,2] · Yanping Sun[1,2] · Ying Liu[1,2] · Yelan Xiao[1,2] · Long Xu[1,2,3] · Tong Shu[1,2] · Xueji Zhang[1,2]

Received: 23 February 2024 / Revised: 7 April 2024 / Accepted: 11 April 2024 / Published online: 6 May 2024

Abstract

Gold nanoclusters (AuNCs) are a class of novel luminescent nanomaterials that exhibit unique properties of ultra-small size, featuring strong anti-photo-bleaching ability, substantial Stokes shift, good biocompatibility, and low toxicity. Various biomolecules have been developed as templates or ligands to protect AuNCs with enhanced stability and luminescent properties for biomedical applications. In this review, the synthesis of AuNCs based on biomolecules including amino acids, peptides, proteins and DNA are summarized. Owing to the advantages of biomolecule-protected AuNCs, they have been employed extensively for diverse applications. The biological applications, particularly in bioimaging, biosensing, disease therapy and biocatalysis have been described in detail herein. Finally, current challenges and future potential prospects of bio-templated AuNCs in biological research are briefly discussed.

Keywords Gold nanoclusters · Bioimaging · Biosensing · Disease therapy · Biocatalysis

Introduction

Gold nanoclusters (AuNCs) refer to a class of sub-nanomaterials consisting of several to hundreds of gold atoms [1–4]. The size of the metallic core of AuNCs is generally less than 3 nm being comparable to the Fermi wavelength of electrons, which results in a quantum confinement effect and leads to unique luminescence properties. Moreover, endowed with the unique surface effects and a high surface-to-volume ratio of AuNCs, the aggregation on the surface of AuNCs can be readily generated, allowing AuNCs to be used in various applications. Nowadays, AuNCs have emerged as a promising candidate for sensing [5, 6], imaging [7, 8], catalysis [9–11] and biomedicine [12, 13]. A variety of strategies including chemical reduction, photoluminescence reduction, and etching, have been developed for the preparation of AuNCs [14, 15]. However, the prepared AuNCs show relatively low stability and quantum yield (QY) of luminescence, which have become the bottleneck of luminescent AuNCs.

In recent years, various ligands have been developed for AuNCs preparation. Researches have demonstrated that appropriate ligands can significantly improve the stability, size control and fluorescence QY of AuNCs [16–19]. Among these ligands, the biological ones, such as amino acids, peptides, proteins and DNA, have received particular attention [12, 20–22]. These biofunctional molecules can not only effectively prevent the aggregation of AuNCs and enhance the fluorescence performance, but also provide the synthesized AuNCs with desirable biological functions [23–25]. There are several recent reviews relating bioligand-protected AuNCs and their biological application, which mainly focus on the methods of tailoring the AuNCs' properties [26], the

Published in the topical collection *Luminescent Nanomaterials for Biosensing and Bioimaging* with guest editors Li Shang, Chih-Ching Huang, and Xavier Le Guével.

✉ Yelan Xiao
ylxiao@szu.edu.cn

✉ Tong Shu
shutong@szu.edu.cn

[1] Shenzhen Key Laboratory for Nano-Biosensing Technology, Research Center for Biosensor and Nanotheranostic, Guangdong Key Laboratory of Biomedical Measurements and Ultrasound Imaging, School of Biomedical Engineering, Shenzhen University Medical School, Shenzhen University, Shenzhen 518060, China

[2] Marshall Laboratory of Biomedical Engineering, Shenzhen University, Shenzhen 518060, China

[3] Department of Gastroenterology and Hepatology, Shenzhen University General Hospital, Shenzhen, China

conformation changes of bioligand [27], or the specific applications in nanomedical fields [26, 28, 29]. This review is organized in a novel way based on the molecular evolution of bioligand, which primarily focuses on the utilization of biomolecules ligands from amino acids to peptides and ultimately to proteins, and from deoxynucleotides to DNA in the preparation of luminescent AuNCs followed by their exploration in bioimaging [30], biosensing [31], disease therapy [32] and biocatalysis [33] (Fig. 1). Besides, some other biomolecules as ligands and the other biological applications are described briefly.

Synthesis of luminescent AuNCs with biomolecules as ligands

The synthetic strategies of biomolecule-protected luminescent AuNCs

Biomolecules such as amino acids, peptides, proteins and DNA have been widely developed as ligands to stabilize AuNCs with unique luminescent properties and improve biocompatibility. Generally, the preparation methods of biomolecule-protected AuNCs can be broadly categorized into the "bottom-up" template method and the "top-down" etching method (Fig. 2) [29, 34]. The former one has become a commonly used method for the synthesis of luminescent AuNCs. In this method, the biomolecules with special configurations and spatial structures are used as templates to provide a stable microenvironment and "model" to fabricate AuNCs. Moreover, the template bioligands can reduce Au^{3+} to Au^{+} and Au^{0} in the synthesis process. For example, Xie et al. [20] have simulated the process of biomineralization in nature, and prepared red-emitting AuNCs@BSA using bovine serum albumin (BSA) as a template via a simple and green route. In addition, phosphorothiolate (ps)-modified DNA has been used as a "model" to prepare AuNCs and it could finely tune the particle size of AuNCs for targeting cellular imaging [35].

The "top-down" etching method refers to the use of relatively large gold nanoparticles (AuNPs) as a precursor material and a suitable etchant to slowly etch the precursor and controllably decrease AuNPs' size, thus obtain luminescent AuNCs. For example, Yang et al. [36] have constructed luminescent AuNCs using bi-phosphorothiolate (ps)-protected AuNPs as precursor and bidentate dihydrolipoic acid as etchant. The results suggested that the etched AuNCs have good stability and enhanced luminescence. In addition, using excess glutathione (GSH) as etchant, the non-luminescent AuNPs have been etched into the small and luminescent AuNCs [37]. The resulting AuNCs showed fluorescent stability in acidic liquid and were useful in the field of sensing and imaging.

Inspired by these two types of synthetic strategies, many novel preparation approaches have been derived from changing the synthesis ligands, steps, environmental conditions and bioligand modification strategies. Thus, a variety of AuNCs incorporated with different biomolecules as ligands have been prepared, which had specific properties and performed excellently in many fields such as bioimaging,

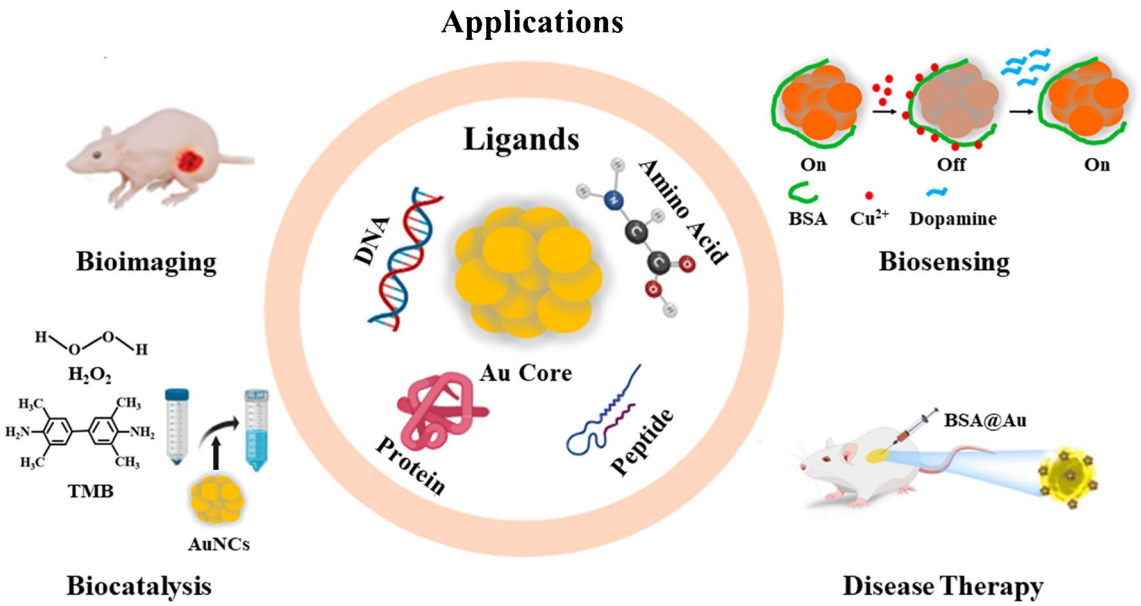

Fig. 1 Schematic illustration of biomolecule-protected AuNCs and their applications

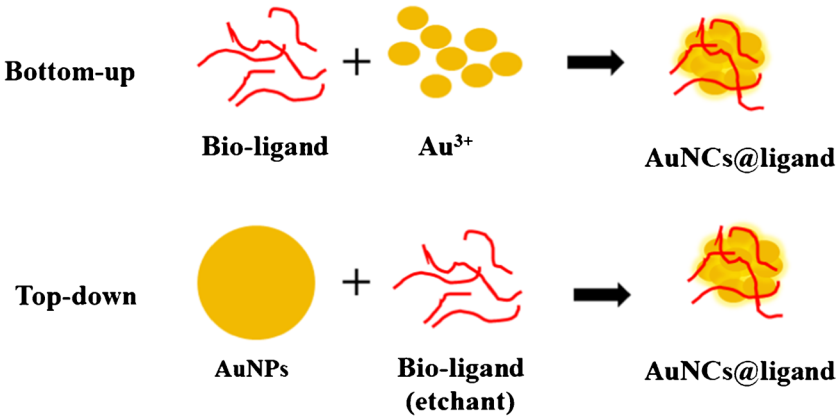

Fig. 2 Schematic diagram of the synthetic strategies of AuNCs

biosensing, biocatalysis and disease therapy as well as other biological fields.

Amino acid-protected luminescent AuNCs

Amino acids, as a class of biomolecules, have a uniform structural formula [38]. Each amino acid has an amino group and a carboxyl group, which allow amino acids having good water solubility, biocompatibility and being easy to combine with other materials. Since most of the amino acids have electron-rich R groups, they can act as Lewis base and nucleophilically react with Au(I) components on the surface of AuNCs to form covalent or coordination bonds, thus stabilize the binding on the surface.

A variety of amino acids with sulfhydryl, non-sulfhydryl groups have been developed as the ligands to fabricate AuNCs. For example, amino acids with sulfhydryl groups (cysteine, methionine) can be stably bound to the gold surface through Au–S bonds to form fluorescent, well-dispersed, and stable AuNCs [20, 39]. Jin et al. [40] have fabricated a series of thiolate-stabilized $Au_n(SR)_m$ with well-defined size and peculiar stability via a kinetically controlled method. Homocysteine with sulfhydryl groups has been used to prepare stable and biocompatible AuNCs by a simple and green method without adding other reducing agents [41]. The prepared AuNCs had orange-yellow fluorescence and were used as fluorescent probes for bioimaging. On the other hand, utilizing cysteine (Cys)-protected AuNCs, a colorimetric detection system for citrate has been developed, to provide a novel method in early diagnosis of prostate cancer [42]. In the present of citrate, the AuNCs@Cys were prohibited to catalyse the oxidation of 3,3′,5,5′-tetramethylbenzidine (TMB), which was the key process of generating blue dye. Furthermore, the system could be applied on paper to detect citrate conveniently. In addition, the methionine (Met) has been introduced as a stabilizing and reducing agent to prepare water-soluble and mono-dispersible AuNCs emitting orange fluorescence [43]. The as-prepared clusters showed selectively and sensitively enhanced fluorescence in the presence of Cd(II) ions with a linear response in the concentration range of 50 nM ~ 35 μM and a detection limit of 12.25 nM for Cd(II) ions. Moreover, this nanoprobe also performed in various environmental, such as water or milk solution. It exhibited satisfactory performance, which indicated the practical applications of this probe.

While amino acids with non-sulfhydryl groups (histidine, lysine, and tryptophan, etc.) can provide amino, imidazolyl, or hydroxyl groups to serve as stabilized groups for the synthesis of luminescent AuNCs [44, 45]. Among this kind of amino acids, histidine not only contains amino and carboxyl groups but also has its unique imidazole group, which can form coordination compounds with Fe^{3+} or other metal ions. Basu et al. [46] have developed a luminescent crystalline inorganic complex, consisting of Zn^{2+} ions and L-histidine plus mercaptopropionic acid stabilized Au_{14}NCs. The resulting compounds were applied for hydrogen sensing as they could reversibly store hydrogen with luminescence at room temperature. The results indicated that the hydrogen adsorption capacity of this complex was 0.244 mM per gram of the complex at 20 °C and 20 bar. Using lysine (Lys) as a template, Xu and coworkers [47] have successfully fabricated highly fluorescent AuNCs@Lys as a fluorescent probe for the detection of Cu^{2+} through a simple one-pot method using reagents of $HAuCl_4$, N_2H_4-H_2O and NaOH. Lys with -NH_2 and -COOH groups linked to Cu^{2+}, and then quenched the fluorescence of AuNCs@Lys. As a result, it was used as a fluorescent sensor with high sensitivity and selectivity for Cu^{2+} detection. Moreover, Lys has also been applied as a ligand to prepare fluorescence nanocomposite probe AuNCs@Lys-MnO_2, which was successfully applied for glutathione (GSH) detection in human serum [48]. In this system, MnO_2 was bind to AuNCs@Lys through electrostatic interaction and quenched the fluorescence of AuNCs@Lys based on fluorescence resonance energy transfer (FRET). Subsequently, MnO_2 would be degraded in the presence of GSH to release the fluorescent AuNCs@Lys, which resulted in partial recovery of fluorescence (Fig. 3).

This probe presented high sensitivity for the detection of GSH with the concentration range of 0.5 ~ 1000 μM and detection limit as low as 5 nM.

Some other amino acids, such as proline [49], tyrosine [50] have also been used as ligands for the synthesis of luminescent AuNCs, which exhibited good selectivity and sensitivity to certain metal ions and were applied to construct corresponding biosensors. Due to the good biocompatibility, low toxicity, and excellent fluorescence properties, amino acids have been exploited as good templates to prepare luminescent AuNCs.

Peptide-protected luminescent AuNCs

Peptides are formed by linking amino acids through peptide bonds and are applied as biological ligands to decorate AuNCs [51, 52]. They contain various functional groups such as amino, sulfhydryl, and phenolic hydroxyl as well as imidazole groups which can stabilize AuNCs by forming stable Au–S [53] or Au–N [54] bonds, and can be used as reducing and stabilizing agents to prepare luminescent AuNCs. Moreover, the surface functionalization of peptides enables the AuNCs to have corresponding or even synergistic biological functions such as sensing, imaging, and disease therapy [55].

GSH, as a common short-chain polypeptide, plays an important role in various physiological functions of the human body and can be used as a ligand coordinating with AuNCs. Various AuNCs with different functions have been fabricated using GSH as a ligand. Wu et al. [56] have synthesized a thermally stable, oxidation-resistant $Au_{25}(SG)_{18}$ via one-pot method, which could readily incorporate specific functionality such as -OH, -COOH, and the atom-transfer radical polymerization initiator $-OC(O)C(CH_3)_2Br$ into the ligand shell of GSH. It offered convenient access to new types of Au_{25} nanoclusters that were difficult to obtain by two-phase approach. In addition, GSH has been used as a reducing agent and ligand to prepare highly luminescent Au-thiolate NCs with the quantum yield to ~ 15% through one-pot synthesis [57]. Using GSH as a ligand endows AuNCs with various advantages in ion detection and biosensing. Well-defined $Au_{25}(SG)_{18}$ protected with GSH have been synthesized and applied to detect Ag^+ based on the fluorescence enhancement, exhibiting a good linear fluorescence response of Ag^+ in the concentration range of 20 nM ~ 11 μM and showing high selectivity among 20 types of metal cations [58]. In addition, GSH-stabilized green-emission AuNCs have been synthesized and applied for sensitive and selective detection of Co^{2+} based on fluorescence bursting [59]. Many other GSH-protected AuNCs have also been developed as optical sensors to detect small biomolecules such as heparin, human trypsin, alkaline phosphatase, and integrins, as well as lysozyme (Lzm) [60, 61].

Compared with natural peptides, synthetic peptides can be designed more readily and play a pivotal role in areas such as sensing and disease therapy. The synthetic antimicrobial peptides (AMPs) are potential materials for antimicrobial therapy. Generally, AMPs include the cationic and hydrophobic segments. The former degrades the negatively charged bacterial membrane, and the latter can be rationally designed to help AMPs insert into infection sites to realize precise therapy. Pranantyo et al. [62] have utilized Cys-terminated AMPs as a reducing ligand to construct AMP-coated AuNCs, which was then functioned with anionic citraconyl (CA) moieties. This AMP-coated AuNCs with CA protection were regarded as a smart design of pH-responsive antimicrobial agents with multiple functions of bacterial imaging, bacterial detection and anti-infection therapy. Apart from the AMPs, the peptides scaffold CCY, consisting of the cysteine (C) and the tyrosine (Y), have

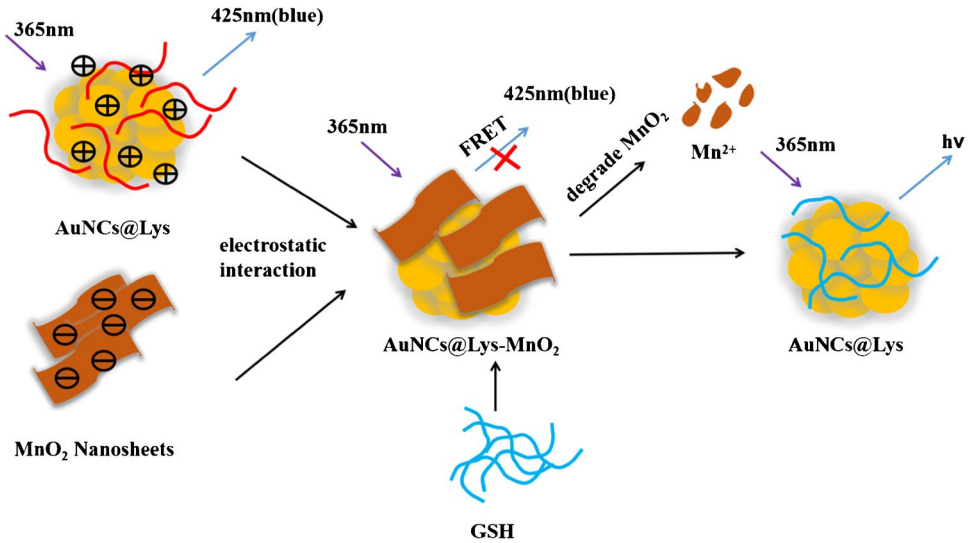

Fig. 3 Schematic illustration of AuNCs@Lys synthesis and the detection principle of GSH

been discovered to be able to capture and reduce Au^{3+}/Au^{+} through the sulfhydryl group of C and phenolic hydroxyl group of Y, respectively. As a result, these CCY-containing peptides have been used to synthesize structurally stable AuNCs that could be utilized for molecular detection. A bifunctional CCYTAT peptide containing a domain of RGRKKRRQRRR with cell nucleus targeting ability and a domain of CCY with the ability to biomineralize and capture Au clusters has been employed to synthesize AuNCs with red emission via a facile method (Fig. 4) [63]. The CCYTAT -AuNCs provided a new choice for specific cell nuclei staining. Some other synthetic peptides containing CCY scaffold such as CCYR9, CCYRKKRRQRRR, CCYSIINFEKL, have also been incorporated into AuNCs to provide unique properties and be employed as biosensors, probes and drug delivery [29, 64–67].

Protein-protected luminescent AuNCs

Protein is one of the six essential nutrients in the human body. It is mainly formed by one or more peptide chains of different lengths folded by disulfide bonding and has a certain spatial structure [68]. Proteins as ligands can be classified into three categories: nutrient proteins, functional proteins, and natural protein matrix. In addition to containing amino and sulfhydryl groups in their amino acid residues, proteins also provide domain-limited space, and hence are one of the key ligands for synthesis of AuNCs [20]. When proteins are used as ligands to synthesize AuNCs, their spatial structure capture Au^{3+}/Au^{+} in situ while the amino acid residues therein act as a reducing agent to stabilize AuNCs as well as a surface modifier [69]. The AuNCs synthesized with various functional proteins as ligands show promising applications in ion detection, sensing, bio-imaging and diseases treatment.

Various nutrient proteins have been employed for the synthesis of AuNCs with high stability and unique fluorescence. BSA is the most commonly used nutrient protein ligand for the synthesis of AuNCs, which not only has a thiol group that can form a stable Au–S bond with gold, but also provides a limited space to prevent the cluster from growing further. Xie et al. [20] have synthesized AuNCs emitting strong red fluorescence via a kinetics-regulated method using BSA as ligand as well as reductant in an aqueous environment at ambient temperature and pressure (Fig. 5). The resulting AuNCs were subsequently found to be highly responsive to Hg^{2+} among complex solution environments [70]. The detection mechanism revealed that the AuNCs underwent fluorescence quenching due to the strong specific interaction between Hg^{2+} and Au^{+}. It demonstrated that this biosensor presented high sensitivity with the detection limit of 0.5 nM (0.1 ppb) for Hg^{2+}, which was much lower than the maximum allowable level of mercury in drinking water (2.0 ppb). Furthermore, Zhang et al. [71] have also applied BSA to synthesize BSA-stabilized AuNCs to successfully monitor the protein hydrolysis activity of trypsin and lactotrypsin in real-time. In addition, BSA possesses abundant binding sites on its shell, which can bind to bio-targeting molecules for cellular imaging, diagnosis and treatment of diseases. It reveals that AuNCs@BSA is a potential candidate for opening up possibilities for further applications.

Functional proteins, such as transport proteins and catalytic proteins, can stabilize AuNCs in combination of decorating them with unique biological functions. Xavier et al. [72] have utilized lactoferrin (LF), a multifunctional transferrin, as a ligand to synthesize luminescent AuNCs that exhibited good stability across a wide pH range of 1 ~ 14. These AuNCs were able to detect the concentration of Cu^{2+} at the parts-per-million (ppm) level. Notably these clusters demonstrated consistent light emission even under varying pH conditions, suggesting their potential for in vivo cellular imaging. Furthermore, these clusters had the potential for molecular delivery owing to the iron-binding and immunomodulatory functions of LF. AuNCs@LF have offered a new therapeutic idea for the treatment of Parkinson's disease [73]. AuNCs modified with LF were efficiently

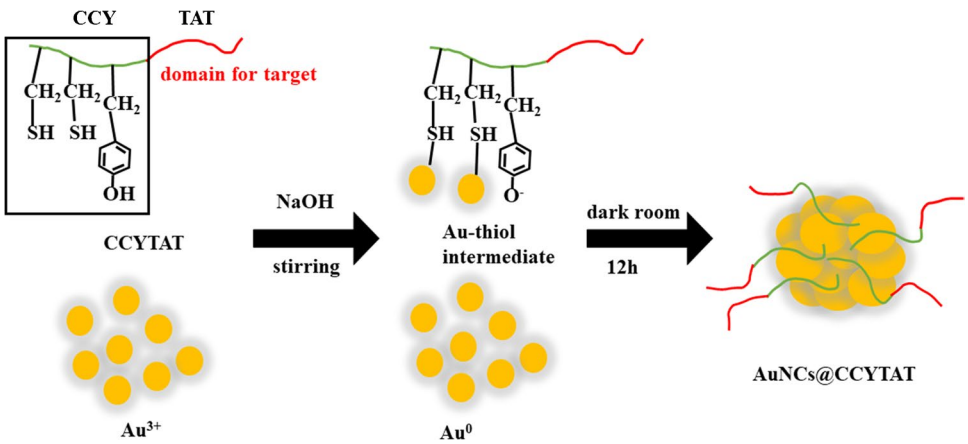

Fig. 4 Schematic illustration of AuNCs@CCYTAT formation

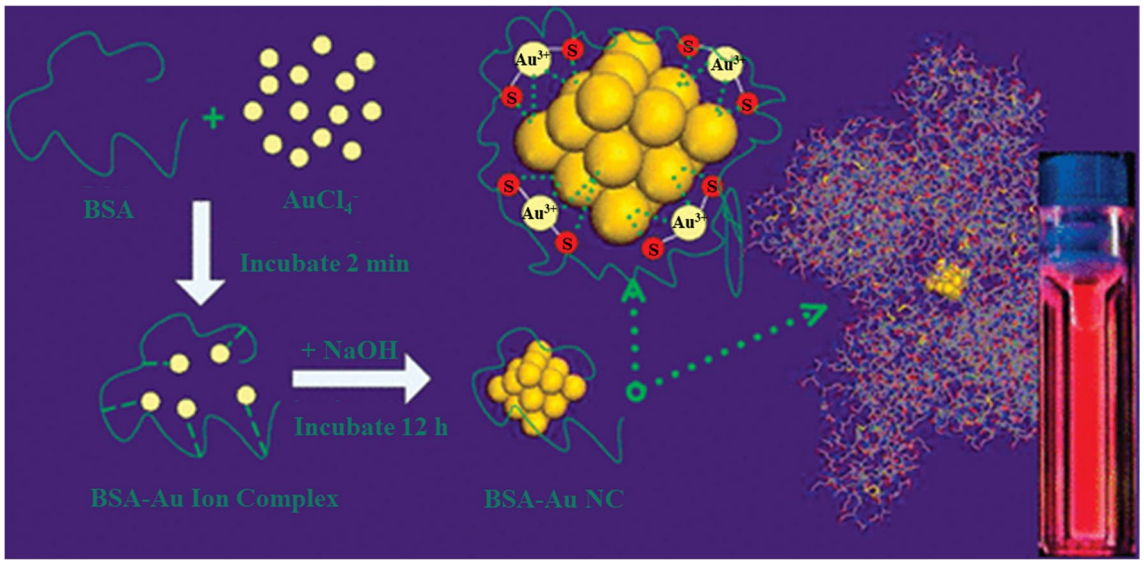

Fig. 5 Schematic illustration of AuNCs@BSA formation. Reprinted with permission from Ref. [20]. Copyright 2009, American Chemical Society

localized in the vicinity of mitochondria. This localization not only protected mitochondria from oxidative stress but also enhanced the blood–brain barrier (BBB) permeability.

Apart from the synthesis of luminescent AuNCs in the protein solution phase, it can also be realized on natural matrix proteins, such as eggshell membranes [74], silk [75], plant protein [76], animal hair [77], etc. This unique synthesis strategy significantly reduces the synthesis cost and enhances the performance of natural matrix proteins, and consequently expands the biological applications of AuNCs. Silkworm silk is a natural protein-based fiber composed with two types of proteins namely firoin and sericin. The outer layer of silk collagen with numerous reducing groups can reduce the Au^{3+}/Au^{+} and the reduction product combine with the silk through Au–S covalent bond subsequntly. Coating AuNCs on the surface of silkworm silk has provided a new idea for the large-scale industrial production of novel silk-based materials through nanotechnology [75]. The "gold silk" prepared by this method exhibited better properties than the original silk, such as enhanced UV resistance and lower in vitro toxicity as well as allergic reaction chances. Feathers and animal hair containing sulfhydryl groups, rich keratin and fibroin proteins can also stabilize AuNCs by reducing Au^{3+} and forming Au–S bonds with gold. Liu et al. [77] have synthesized water-soluble luminescent AuNCs by a one-step method using wool keratin (WK) and silk fibroin (SF) as stabilizers and reducing agents. They found that the ratio of WK and SF proteins would affect the fluorescence intensity of AuNCs. In addition, keratin from goose feathers has been employed as a stabilizer and reducing agent to synthesize red fluorescent AuNCs [78]. These AuNCs were etched to form Au(I) complexes with aggregation-induced emission (AIE) activity, which could be induced by Cd^{2+} to produce strong luminescence. Permanent fluorescent hair coloring has emerged as a contemporary method of hair coloring, catering to the growing desire for uniqueness and style. The luminescent AuNCs as fluorescent hair dyes have been embedded into the hair by a rapid protein-assisted biomineralization method under heating and alkaline conditions [79]. The hair scales were fully opened, enabling the dye precursors to penetrate deeply under the optimal temperature and alkalinity. The introduction of AuNCs gave new photophysical properties to the hair and greatly enhanced its antistatic, mechanical strength, durability, and biocompatibility.

DNA-protected luminescent AuNCs

DNA contains four nitrogenous bases: adenine A, thymine T, guanine G, and cytosine C, having deoxyribose and a phosphate group (Fig. 6) [80]. Hydrophilic phosphate group carries an abundance of electrons, while keto and imine groups in the bases having strong tendency to bind with metal ions. These structural advantages enable the nucleotides to capture Au^{3+}/Au^{+} by physical adsorption or chemisorption as AuNCs synthesis occur under mild reducing agents [81]. Using a series of adenine derivatives as ligands under citrate reduction, AuNCs with different fluorescence intensity have been synthesized [82].

Free deoxyribonucleotides are connected by phosphodiester bonds to form single-stranded DNA [83]. Single-stranded DNA molecules possess specific base pair recognition ability, high biodegradability as well as biocompatibility, and their nitrogenous bases and negatively charged backbone provide numerous binding sites for Au^{3+}/Au^{+} through electrostatic

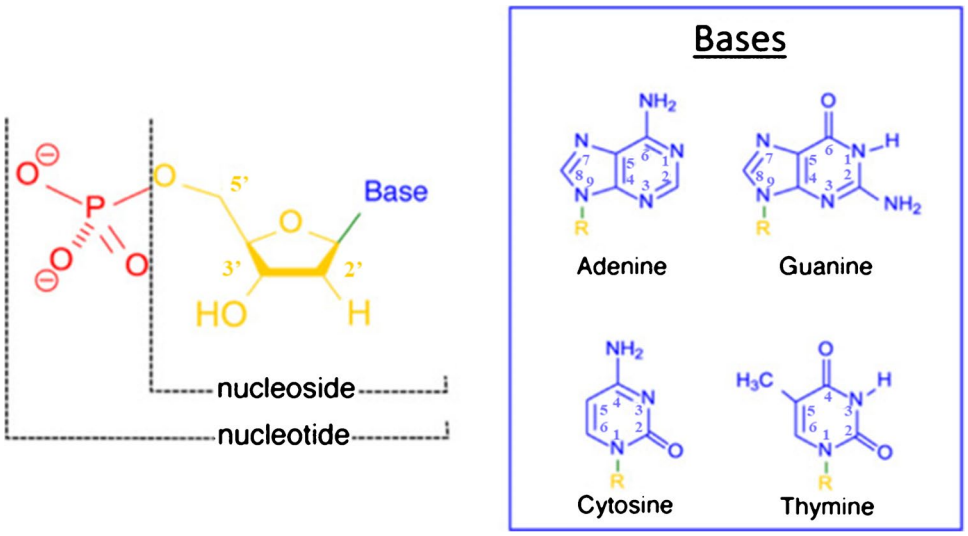

Fig. 6 Schematic illustration of DNA's structure. Reprinted with permission from Ref. [80]. Copyright 2017, Wiley–VCH

or liganding effects [84]. They have become popular ligands for the synthesis of luminescent AuNCs performing well in gene detection [85], bio-therapy [86], bio-sensing [87], and other areas.

Currently, the mainstream ligands for synthesizing AuNCs are still mainly hydrophobic ligands with limited solubility in water, hindering the application of AuNCs in physiological environments. Gold ions are captured by hydrophilic macromolecular DNA through electrostatic adsorption and Au–N and Au-O interactions [88]. These gold ions are then arranged along the DNA backbone and synthesized into AuNCs with the help of mild reductants. Compared with the hydrophobic ligands, using hydrophilic ligands to synthesis fluorescence AuNCs is more complex. The length, sequence, and spatial configuration of the DNA strand, the acidity and alkalinity of the reaction environment as well as the type of reductant, jointly affect the fluorescence properties and intensity of the synthesized AuNCs. Under dimethylaminoborane (DMAB) reduction and using four base-corresponding poly-deoxyribonucleotide strands as ligands respectively, the effect of DNA sequence on the luminescence intensity of AuNCs has been investigated [89]. The findings revealed that the luminescence intensity of the synthesized clusters exhibited a decreasing trend as 23-C > 23-A > 23-T > 23-G. Additionally, the maximum emission wavelengths also undergent blue-shift in the same order. Subsequently, the same team used DMAB as a reducing agent and hairpin-structured, single-stranded, as well as double-stranded DNA as templates to investigate the effect of spatial configuration of DNA sequences on the emission behavior of AuNCs (Fig. 7) [90]. The double-stranded DNA was structurally inefficient compared to hairpin-structured and single-stranded DNA, which did not favor the binding growth of AuNCs. Hairpin-structured DNA captured Au^{3+}/Au^{+} and facilitated the synthesis of reddish-glowing AuNCs under the action of the ring-containing carbon chain structure and the reducing agent. The luminescence intensity was highly dependent on the ring sequence, with the cytosine ring (C5) being the most efficient host. Compared with single-stranded DNA, the hairpin structure of DNA was less prone to coil proximal and distal bases randomly, which better elucidated the effect of sequence on the luminescent properties of AuNCs. Using citrate as a reducing agent, the effect of pH as well as other various buffer conditions on the synthesis of AuNCs have been investigated. It was reported that AuNCs with blue fluorescence could be prepared in the presence of poly-cytosine DNAs at low pH and poly-adenine at neutral pH. In addition, Lopez and coworkers [91] have investigated the effect of reducing agents on the synthesized luminescent AuNCs using poly-deoxyribonucleotide as a ligand. Apart from the widely used citrate and DMAB, potent reducing agents such as 4-(2-hydroxyethyl)-1-piperazineethanesulfonic acid and its sodium salt (HEPES) as well as 2-(N-morpholino)ethanesulfonic acid (MES) were also employed. Compared to these reducing agents, AuNCs@DNA reduced by the strong reducing agent $NaBH_4$ had no fluorescence.

For the synthesis of DNA-protected AuNCs, in order to overcome the electrostatic hindrance of luminescent AuNCs' surface ligands exchanging with DNA, several strategies for in situ DNA-functionalized AuNCs have been developed based on DNA's affinity for positively charged substances or the formation of stronger bonds between modified DNA and gold. Wang et al. [92] have utilized peptide K4 (KRKC-NH_2, a tetrapeptide) to modify the AuNCs with positively charged surface and make it easy to assemble with DNA strands to form complex nanostructures. Besides, phosphorothioic acid-modified DNA (ps-DNA) has also been utilized as a ligand to enhanced the DNA's affinity for gold and to synthesize valence-controllable AuNCs in situ [35]. The size

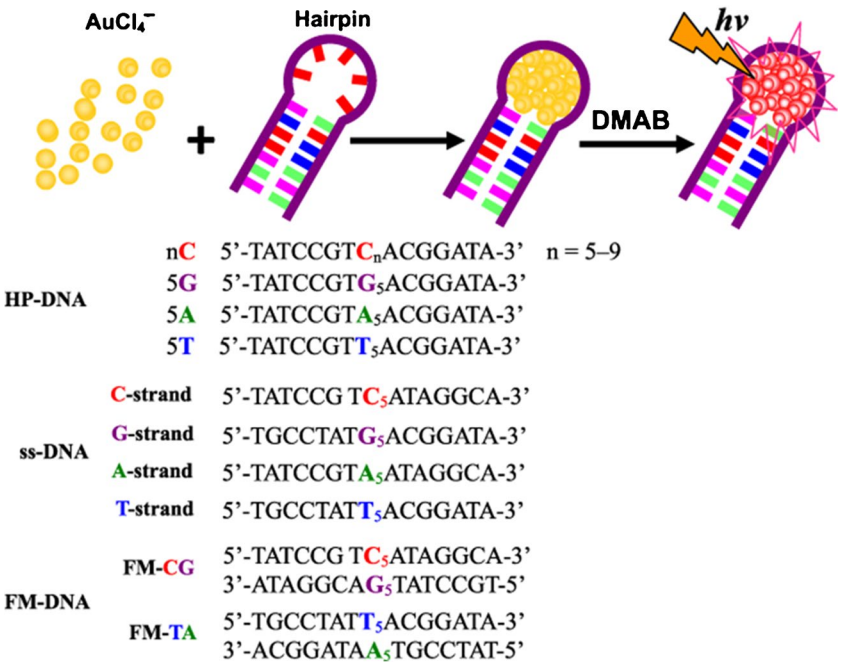

Fig. 7 Schematic illustration of red emitting AuNCs conformed by hairpin-structured DNA. Reprinted with permission from Ref. [90]. Copyright 2012, IOP Publishing Ltd

of the resulted AuNCs was finely adjusted in the range of 1.3 ~ 2.6 nm by adjusting the ps-DNA length. Apart from the advantage of making AuNCs to be size-controlled, ps-DNA also contained a functional recognition domain, which could be designed to specifically recognize small molecules through base complementary pairing. These studies provide a new idea for the assembly and functionalization of novel luminescent AuNCs with DNA.

Other biomolecule-protected luminescent AuNCs

The biomolecules of amino acids, peptides, proteins and DNA have been proved to be promising ligands for the synthesis of fluorescent AuNCs. Compared to these ligands, other biomolecules such as cellulose [93], chitosan [94] and biosurfactant (sodium cholate) [95] have also been employed for the synthesis of AuNCs. Cellulose is one of the largest natural polymers with biocompatibility, biodegradability and a capability to scatter low-visible light. Cellulose with nano size can form a nanoscale dispersion in water to form interparticle hydrogen bonds that promote network formation and prevent self-aggregation. Using cellulose crystal (CNC) as carriers and stabilizers, a ratiometric fluorescent probe based on CNC-protected AuNCs was fabricated for live-cell and zebrafish imaging of highly reactive oxygen species (ROS). Chitosan is a natural cationic biopolymer synthesized from alkaline N-deacetylation of natural chitin with amino and hydroxyl group in each repeating unit. Chitosan has good biodegradability, biocompatibility and low cytotoxicity, which is a promising material for the decoration of AuNCs. For example, chitosan grafted with N-acetyl-L-cysteine (NAC-CS) was prepared and used to synthesize AuNCs@NAC-CS with biocompatibility, good fluorescence, low cytotoxicity, and low sensitivity to some content of living cells. In addition, other biosurfactant (sodium cholate) was applied as template to fabricate bright bluish-green emitting AuNCs by a green chemical approach for in vivo bioimaging in zebrafish embryos. Compared to the commonly used bioligands with amino acids, peptides, proteins and DNA, the other biomolecule-stabilized AuCNs have been less reported.

Summary of different biomolecule-protected luminescent AuNCs

Biomolecules (amino acids, peptides, proteins and DNA, etc.) are demonstrated to be promising templates for the fabrication of multifunctional fluorescent AuNCs. The biotemplates can not only act as ligands to improve the stability, biocompatibility and sensitive optical properties of AuNCs, but also enable the AuNCs having biological activity and low toxicity. For example, though amino acid has the simplest structure and function, it possesses some important groups like sulfhydryl groups, amino, imidazolyl, or hydroxyl groups, which are able to stabilize AuNCs through strong Au–S bonds and reduce AuNCs without any other reduction. Furthermore, amino acid, with stable and definite structure, has been employed to fabricate atomically precise AuNCs [96].Compared to amino acids, peptides and proteins are complex and have abundant active functional groups to make protein-protected AuNCs outstanding among other AuNCs. Benefited from peptide synthesis engineering, designing

specific-function peptide is possible. The natural functional protein, such as, enzyme and transport proteins, can decorate AuNCs with special biological functions for biomedical applications including biosensing, bioimaging, biolabeling, targeted cancer therapy and drug delivery. In some respect, the peptide or protein-functionalized AuNCs are preferable to conventional fluorescent probes due to the good stability, excellent compatibility, and prolonged fluorescence lifetime [97, 98]. Compared with hydrophobic ligand, hydrophilic macromolecular DNA endows AuNCs with gene detective ability as well as solubility in physiological environment. Despite many advantages of using biomolecule as template for AuNCs, in some extent, their luminescence is relatively weaker comparing to the conventional fluorescent dyes or quantum dots, which limits their applications. However, as the biomolecules become more complex, it is believed that more novel biomolecules and synthesis strategies would be developed to fabricate enhanced luminescent AuNCs to realize biological applications in changeable complex physiological environment.

Major biological applications

With the advantages of biodegradability, biocompatibility, low cytotoxicity, large Stoke shifts and unique luminescence properties, biomolecules (amino acids, peptides, proteins and DNA) protected AuNCs have emerging as promising candidates in various fields, especially in biological applications including bioimaging, biosensing, disease therapy and biocatalysis, etc.

Bioimaging

In vitro bioimaging

Templates, such as amino acids, peptides, proteins and DNA, for fluorescent AuNCs have been widely applied in cell targeting imaging and metabolism studies in living cells. Folic acid (FA) serves as a bio-probe that facilitates the entry of substances into cells effectively. Modifying FA ligand with green-emitting fluorescein isothiocyanate (FITC), Ding et al. [99] have prepared an AuNCs-based fluorescence biosensor (FA-FITC@AuNCs) for specific bioimaging in cancer cells and ratiometric determination of intracellular pH. The obtained biosensor exhibited excellent sensitivity, high cyclic accuracy and good selectivity over various metal ions and biological species in a broad pH range of 6.0 ~ 7.8. It was also successfully applied in targeted imaging for FR^{+ve} Hela cells and FR^{-ve} lung carcinoma cells A549. Hada et al. [100] have also used FA to functionalize BSA-AuNCs for targeted fluorescence imaging of ovarian cancer cells (NIH:OVCAR-3). Compared to the BSA-AuNCs, the FA-functionalized BSA-AuNCs possessed good biocompatibility and improved cellular uptake and staining ability. This research suggested that the synthesized FA-BSA-AuNCs could act as an efficient label-free contrast agent for early cancer diagnosis by cellular imaging. Retnakumari et al. [101] have used BSA as a template and ascorbic acid as a reducing agent to fabricate novel AuNCs. FA could attach to the BSA protein via a coupling agent and the FA-BSA-AuNCs could be attached to oral cancer cells as fluorescent markers. Bhamore et al. [102] have created the viability of BSA-bromelain-AuNCs as a fluorescent probe for imaging of fungal cells. In addition, Bertorelle and coworkers [103] have introduced BSA to functionalize the surface of water-soluble thiolated Au_{25}NCs. With the attachment of BSA, the AuNCs exhibited a significant enhancement of photoluminescence and a redshift in the near infrared II (NIR-II) window. This study provided a new strategy to tailor sensitive probes with NIR-II photoluminescence via selectively binding protein onto the AuNCs for the optical detection of biomolecules in a cellular environment by living imaging.

GSH serves as a reducing agent and ligand to construct fluorescent AuNCs for live cell imaging, allowing the real-time monitoring of changes in the intracellular environment [104]. Sun et al. [105] have synthesized GSH-protected AuNCs with fluorescent emission wavelength of 800 nm and they demonstrated that the GSH-AuNCs can be used for bioimaging of targeted tumor cells. The fluorescence intensity of GSH-AuNCs presented a reversible linear temperature response and the addition of FA would not affect the fluorescence peak. $Au_{25}(SR)_{18}$ is the most studied AuNCs structure and has shown good stability and dispersion property in many studies. Liu et al. [106] have developed a water-soluble and photostable $Au_{25}(GSH)_{18}$ cage structure with a fluorescent emission in the range of 1120 ~ 1350 nm. The quantum yield of this $Au_{25}(GSH)_{18}$ was greatly increased by metal-atom doping on its surface, which allowed penetration into the skull for NIR-II cerebral blood vessel imaging. Using principal component analysis techniques, the primary tumor, blood vessel, and lymphatic metastasis could be clearly distinguished via cancer metastasis imaging (Fig. 8A). Li et al. [107] have constructed a GSH-stabilized $Au_{25}(GSH)_{18}$ with a blue-shifted fluorescence mission at 1050 nm. $Au_{25}(GSH)_{18}$ attached efficiently to hydroxyapatite (the main component of bone), resulting from the specific binding between the carboxyl group at the end of the GSH ligand in $Au_{25}(GSH)_{18}$ and Ca in hydroxyapatite. The whole mouse body exhibited a vital NIR-II fluorescence within 8.5 min after $Au_{25}(GSH)_{18}$ injection. As the time was extended, the $Au_{25}(GSH)_{18}$ would remarkably decrease and its signal became weak in other body parts apart from in skeletal sites with enhanced signal. After 8.3 h of injection, almost all skeletal structures showed clear fluorescence (Fig. 8B). It indicated that this nanocluster was an excellent

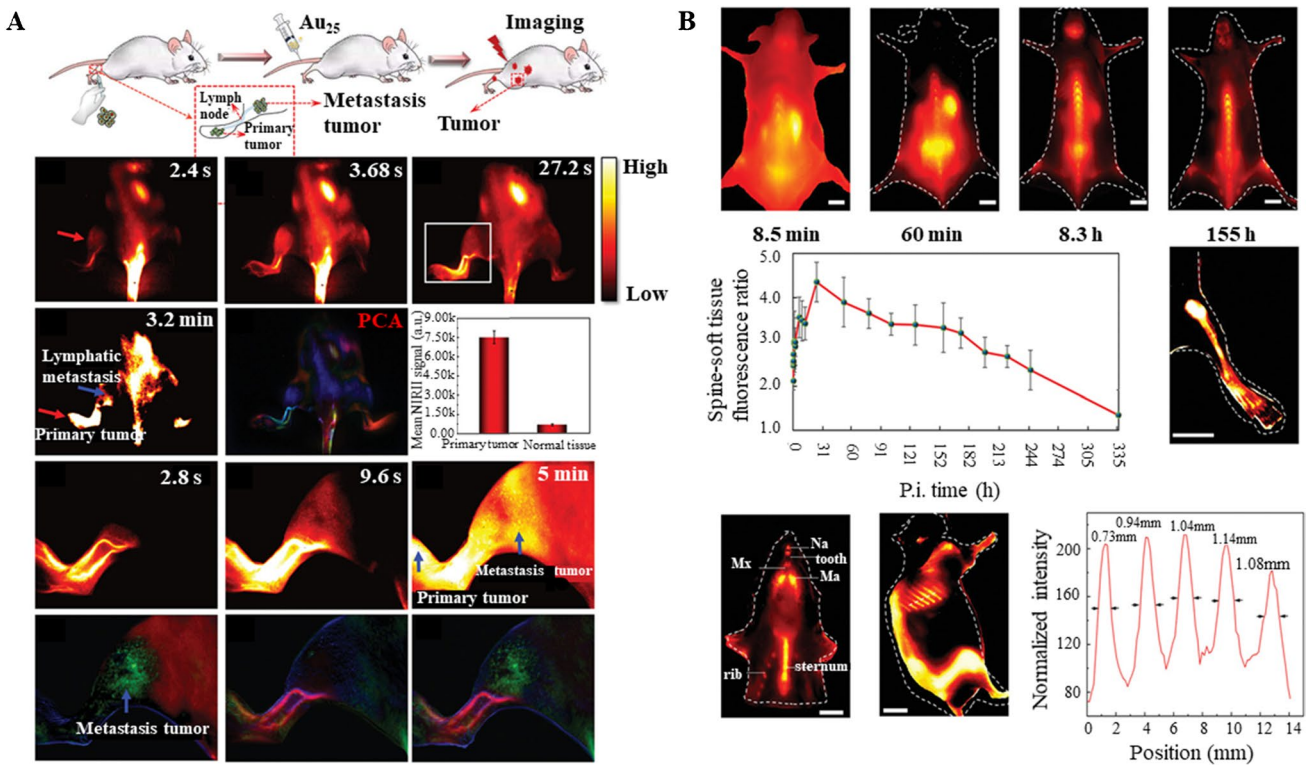

Fig. 8 (**A**) NIR-II fluorescence imaging of tumor metastasis through the intravenous injection of $Au_{25}(GSH)_{18}$ and primary tumor, blood vessel, and lymphatic metastasis are distinguished. Reprinted with permission from Ref. [106]. Copyright 2019, WILEY-VCH. (**B**) Specific bone targeting and high resolution NIR-II fluorescence imaging of the whole mouse body. Reprinted with permission from Ref. [107]. Copyright 2020, Wiley-VCH

NIR-II bone imaging probe and had great potential for fluorescence-guided skeletal surgery. Many other imaging probes based on GSH-AuNCs have been created and showed promising materials for biological applications [108–110]. Apart from the aforementioned BSA- or GSH-protected AuNCs-based nanoprobes, other novel fluorescent nanoprobes have been designed. For example, a photoswitchable fluorescent nanoprobe towards dual-color cellular imaging has been fabricated using ligand-protected AuNCs [111]. In this nanoprobe system, the AuNCs did not only act as FRET donors due to their intrinsic fluorescence properties, but also played a vital role in tuning the photochromic and aggregate properties of spiropyran via ligand-spiropyran interactions.

In vivo bioimaging

As a powerful technique, in vivo imaging can localize and dynamically monitor biomolecules in living systems. Water-dispersible AuNCs with NIR emission are ideal candidates for in vivo imaging due to their higher penetration capacity and biocompatibility. Wu et al. [112] have explored a novel contrast imaging agent based on BSA-modified AuNCs for tumor fluorescence imaging in vivo. The fluorescence signal of AuNCs in living organisms could be clearly distinguished and it showed high photostability, allowing continuous imaging in vivo. Using MDA-MB-45 and Hela tumor xenograft models, in vivo tumor targeting studies showed that BSA-AuNCs would highly accumulate in tumor sites due to the enhanced permeability and retention (EPR) effect. It demonstrated that this nanomaterial was a promising contrast imaging agents for in vivo fluorescence tumor imaging. Xu et al. [113] have also used BSA as template to prepare BSA-AuGd integrated nanoprobes for optical/MRI/CT triple-modal in vivo tumor imaging. This nanomaterial owned good biocompatibility, quick degradability and nontoxicity to normal tissue in vivo. Another fluorescent BSA-protected AuNCs have been fabricated via the surface modification of BSA-AuNCs with Met and MPA, the AuNCs could achieve targeted imaging of MDA-MB-231 tumors in living cells [114]. Wang et al. [115] have developed novel probes based on BSA-AuNCs with good X-ray absorptive capacity, which were used for the 2D and 3D live imaging of murine kidneys. GSH can also be explored to fabricate AuNCs for in vivo imaging. For example, Yang et al. [116] have prepared GSH-protected AuNCs appearing as a novel neurofluorescent probe.

Apart from BSA and GSH, other biomolecules have also been developed as templates to synthesize AuNCs for in vivo imaging. Using one-step microwave-assisted method, Li et al. [30] have synthesized lysozyme-protected AuNCs (Lzm-AuNCs) with good biocompatibility, stability and red fluorescence, as well as low toxicity. After injection into the living cells, Lzm-AuNCs would be almost located lysosomes. Lzm-AuNCs could selectively and sentitively drive the detection of folate with a detection limit of 0.19 nM. Moreover, the hyaluronic acid (HA) coated Lzm-AuNCs showed significant targeting to tumors. This study indicated that Lzm-AuNCs could serve as sensing, in vivo fluorescence imaging and tumor targeting (Fig. 9A). Pang et al. [117] have synthesized dual-ligand/multi-ligand-coated AuNCs for specific targeting, NIR fluorescence imaging, diagnosis and treatment of lymph-node (LN) cancer metastasis in in vivo mouse models. $Au_{25}(SR_1)_n(SR_2)_{18-n}$ with highly effective LN targeting, good biocompatibility and stability and optimal body-retention time, could be obtained via optimization of the coating ligands. The Au nanomaterials exhibited bright NIR-II fluorescence, and more stable and friendly than ICG (a commonly used commercial LN imaging agent) (Fig. 9B). Compared to visible and NIR-I emission (400 ~ 800 nm), NIR-II emission (1000 ~ 1700 nm), exhibiting a longer wavelength and less light scattering, enables the clear imaging of deeper organisms and tissues possibly. Biomolecule-protected AuNCs with fluorescence emission in the NIR-II window have attracted substantial research interest for bioimaging [118]. In addition, ribonuclease-A (RNase-A) has been utilized to encapsulate AuNCs (RNase-A@AuNCs) for red-shifted emissions because it contains a desired cocktail of thiol group (Cys) and aromatic amino acids (histidine and tyrosine). The in vivo imaging capability of RNase-A@AuNCs in gastrointestinal imaging (GI) tract was investigated in mice by oral administration. This work demonstrated that RNase-A@AuNCs could be applied as nano-emitters for diagnosis of intestinal tumors [119].

Biosensing

Due to the unique fluorescent and physicochemical properties, a variety of biomolecule-protected AuNCs have already been developed for biosensing probes for detection of metal ions, small organic molecules, amino acids, polypeptides and proteins, etc. Compared to conventional organic labels, fluorescent biomolecule-coated AuNCs have the advantages of high sensitivity, excellent photostability and aqueous solubility. A list of recent advances in biomolecule-coated AuNCs and their bioconjugates is summarized in Table 1.

Fluorescent AuNCs have been widely introduced to detect metal ions such as Hg^{2+}, Cu^{2+}, Cd^{2+}, Fe^{3+}, Ag^{+}, Co^{2+}, etc. Hg^{2+} is becoming a threat to the environment and human beings due to its highly hazardous and bio-accumulative properties. Many Hg^{2+} detection approaches have been investigated. For example, Xie et al. [70] have developed a BSA-coated AuNCs via a simple label-free method for the determining Hg^{2+}. The presence of Hg^{2+} would quickly quench the fluorescence of BSA-AuNCs within a second due to the strong-affinity metallophilic Hg^{2+}-Au^{+} interactions. As clearly indicated from the photoemission spectra (Fig. 10A), this protocol showed high selectivity and sensitivity towards Hg^{2+} with the detection limit of Hg^{2+} up

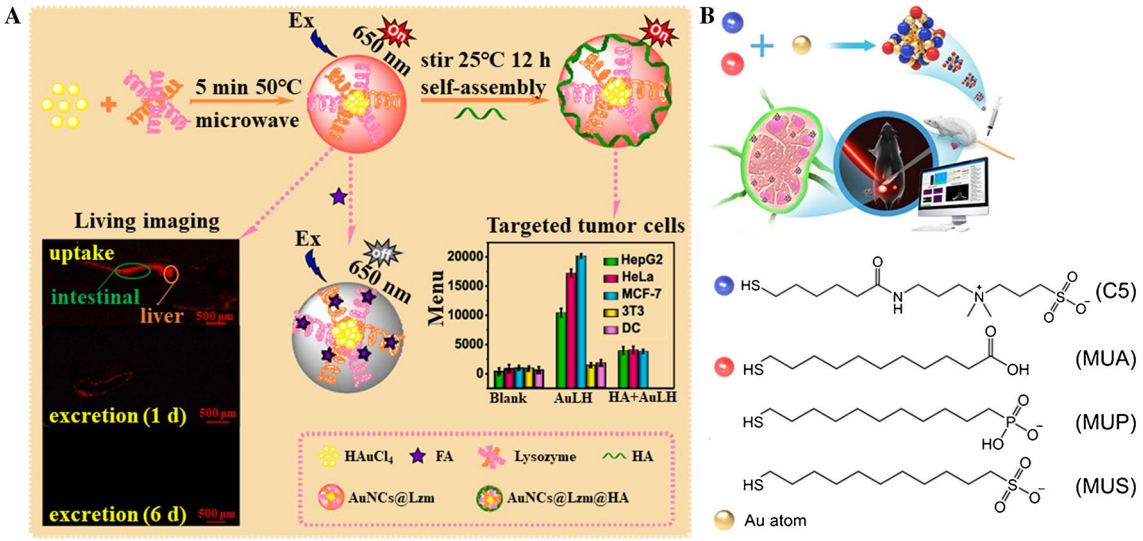

Fig. 9 (**A**) Formation of Lzm-AuNCs and the applications in tumor cells targeted and in vivo living imaging. Reprinted with permission from Ref. [30]. Copyright 2022, Elsevier. (**B**) Formation of dual-ligand-coated AuNCs and the NIR-II fluorescence of AuNCs used in vivo imaging. Reprinted with permission from Ref. [117]. Copyright 2022, Pang. et al. Published by American Chemical Society

Table 1 Analytical applications of AuNCs for sensing

Ligand	$\lambda_{ex}/\lambda_{em}$ (nm)	Size (nm)	Analyte	Linear range(μM)	LOD (nM)	Ref
Lysine	338/418	~3.0	Cu^{2+}	0.01 ~ 7	3	[47]
DNA	370/455	~4.0	Cu^{2+}	0.5 ~ 80	500	[121]
Insulin	365/490	2.0 ± 0.8	Cu^{2+}	0.05 ~ 1.70	7.5	[122]
BSA	470/640	~1.0	Hg^{2+}	0.001 ~ 0.02	0.5	[70]
BSA-GO	470/635	~8.0	Hg^{2+}	0.01 ~ 0.2	0.0238	[120]
Methionine	420/565	1.5 ~ 2.0	Cd^{2+}	0.05 ~ 35	12.25	[43]
L-proline	360/440	~2.0	Fe^{3+}	5 ~ 2000	2000	[49]
GSH	514/670	~2.0	Ag^{+}	0.02 ~ 11	200	[58]
Lysine	338/425	3 ± 0.5	GSH	0.5 ~ 1000	5	[48]
Insulin	365/490	2.0 ± 0.8	GSH	0.05 ~ 1.50	9.2	[122]
Cysteine	365/630	4.0 ~ 6.0	Citrate	0.5 ~ 1000	100	[42]
L-tyrosine	385/470	1.0 ~ 3.0	Tyrosinase	0.5 ~ 200	80	[50]
HSA	365/670	~5.0	Nitrite	0 ~ 20	46	[124]
BSA-Cu^{2+}	365/635	~1.8	Pyrophosphate ion	0.16 ~ 78.1	83	[125]
BSA-Ce	325/410,658	-	CN^{-}	0.1 ~ 15	50	[126]
BSA	480/622	~2.82	Dopamine	0 ~ 3.5	10	[127]
BSA	370/629	~2.0	Folic acid	75 ~ 272	40	[129]
LTN	375/470	~3.2	Oxytetracycline	0.5 ~ 15	300	[132]

to 0.5 nM, 20 times less than the United States Environmental Protection Agency safe limit for Hg^{2+} in drinking water. Yu et al. [120] have prepared a novel BSA-AuNCs with combination of graphene oxide (GO) hybrid membrane to achieve the detection and separation of Hg^{2+} effectively (Fig. 10B). It demonstrated that the effective separation of Hg^{2+} resulted from the intense interaction of Hg^{2+}-Au^{+}, the specific binding of Hg^{2+} and the Cys residue of BSA

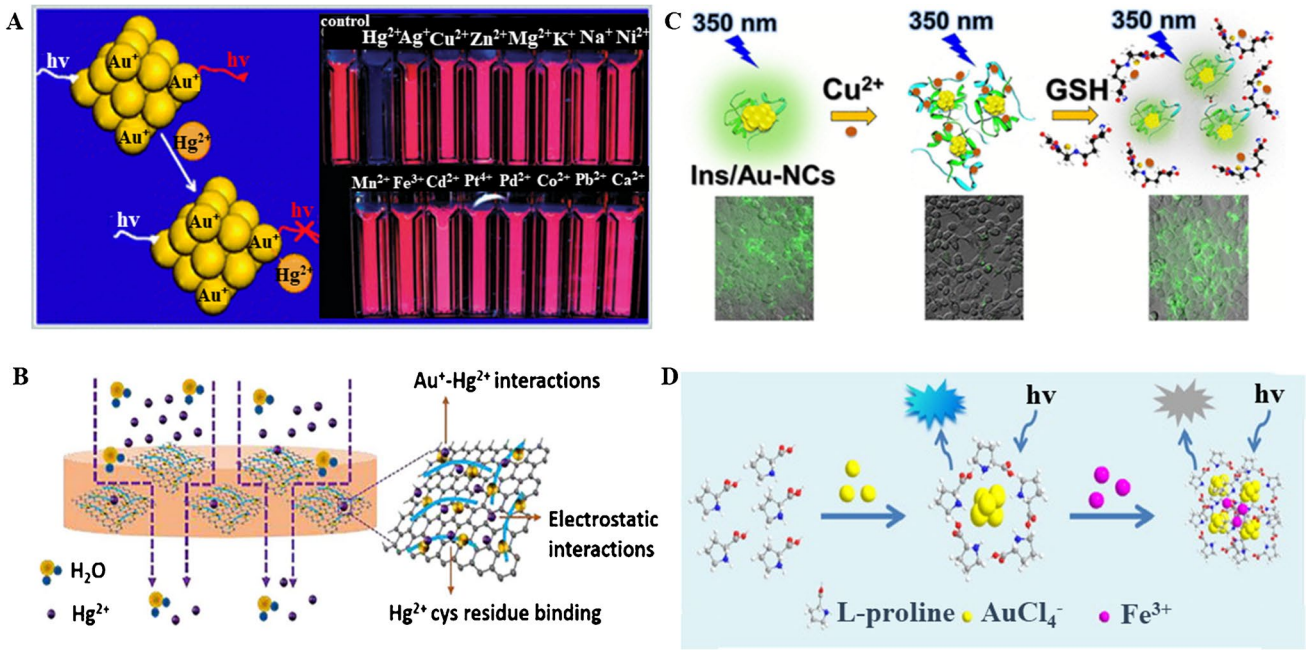

Fig. 10 (**A**) Detection of Hg^{2+} with BSA-AuNCs. Reprinted with permission from Ref. [70]. Copyright 2010, Royal Society of Chemistry. (**B**) Detection of Hg^{2+} using BSA-AuNCs with combination of GO hybrid membrane. Reprinted with permission from Ref. [120]. Copyright 2018, Elsevier. (**C**) Detection of GSH and Cu^{2+} with insulin-capped AuNCs. Reprinted with permission from Ref. [122]. Copyright 2023, American Chemical Society. (**D**) Synthesis of L-proline-stabilized fluorescent AuNCs and the application for Fe^{3+} detection. Reprinted with permission from Ref. [49]. Copyright 2013, Elsevier

as well as the electrostatic interaction. Over-accumulation Cu^{2+} will cause toxicity and bring serious diseases to human beings. Currently, biomolecule-modified AuNCs have been fabricated for the detection of Cu^{2+} [47, 121, 122]. Shamsipur et al. [122] have developed an on-off-on fluorescence probe based on green-light-emitting insulin-capped AuNCs for rapid, sensitive and selective detection of Cu^{2+} ions and GSH (Fig. 10C). The fluorescence intensity of these nanoclusters was significantly decreased by Cu^{2+} resulting from an aggregation-caused quenching, while it could be recovered by addition of GSH. The detection limits for Cu^{2+} and GSH were ~ 7.5 and 9.2 nM, with linear ranges of 0.05 to 1.7 μM and 0.05 to 1.5 μM, respectively. Some other bioligands including Lys [47] and DNA [121], have also been applied for the synthesis of AuNCs for the determination of Cu^{2+}. In addition, novel water-soluble Met-capped AuNCs have been synthesized by a green and facile method, and used as a fluorescence-enhanced probe for Cd^{2+} sensing with a linear response in the range of 50 nM to 35 μM and a detection limit of 12.25 nM [43]. The fluorescence of the Met-AuNCs was selectively and sensitively enhanced in the presence of Cd^{2+} attributed to the Cd^{2+}-induced aggregation of nanoclusters. Mu et al. [49] have synthesized L-proline-stabilized fluorescent AuNCs serving as sensing probes for serum iron based on the aggregation-induced fluorescence quenching (Fig. 10D). Biomolecule-functionalized AuNCs are also utilized for determination of other inorganic ions such as citrate [42], sulfide [123], nitrite [124], pyrophosphate [125] and cyanide [126].

Fluorescent AuNCs can be also used for the sensing of small molecules. Aswathy et al. [127] have developed a fluorescence "turn on" sensor to detect dopamine (DA) using Cu^{2+}-decorated BSA-AuNCs. The fluorescence of BSA-AuNCs was initially quenched by Cu^{2+}, and recovered by the introduction of DA due to the conformity between Cu^{2+} and the amino group of DA (LOD: 0.01 μm). Novel BSA-functionalized AuNCs have been fabricated for detection of acetylcholine [128], folic acid [129], glutaraldehyde [130], cholesterol [131] with excellent selectivity and sensitivity. Moreover, the biomolecule-protected AuNCs have also been employed for the amino acids, peptides, proteins sensing. L-tryptophanonitrile (LTN)-protected AuNCs (LTN@AuNCs) have been successfully fabricated and applied to detect oxytetracycline via colorimetric analysis based on their enzyme-like activity [132]. Oxytetracycline caused the aggregation of positively charged LTN@AuNCs with the negatively charged drug, and then the aggregated LTN@AuNCs would produce more ROS and improve their peroxidase (POD)-like activity. As a result, a colorimetric technique for the detection of oxytetracycline with high specificity and sensitivity was developed. This method exhibited the detection limit of 0.3 μM and a good linear relationship for ultraviolet–visible absorbance of the aggregated LTN@AuNCs at a wavelength of 650 nm with oxytetracycline in a range of 0.5 ~ 15.0 μM ($R^2 = 0.994$). Apart from these studies, an alternative method, known as "chemical nose-tongue" strategy, has been investigated on sensing protein. Yu et al. [133] have prepared a novel fluorescent probe in the sensing array by the integration of seven fluorescent probes with GO. This assay was capable of identifying different proteins at different concentrations (47 out of 50 different proteins with accuracy of 94%) due to the interactions between GO and the fluorescent probes.

Biomolecule-functionalized AuNCs have also gained substantial attention for ratiometric fluorescent probes due to their prospective potential in biosensing and bioimaging [134, 135]. Peptide-protected (GSH) and protein-protected (BSA, lzm) AuNCs show red-emitting property in NIR, which has low absorption and autofluorescence from tissues and organisms [136]. Therefore, peptide-protected and protein-protected AuNCs are widely attractive in living cell biosensing and bioimaging. Modified GSH-capped AuNCs with green-emitting FITC molecules, the FITC-GSH-AuNCs exhibited dual emission peak at 520 nm and 675 nm, among which the red emission signal was sensitive to the Hg^{2+} while the green fluorescence peak was constant [31]. Furthermore, the ratiometric fluorescent probe has realized sensing and imaging of Hg^{2+} changes in living cells and zebrafish. In addition, FITC has also been conjugated with the amino groups of BSA-capped AuNCs, and the compound emitted at 525 nm and 670 nm achieving sensitive detection of solution pH and H_2O_2 [137]. Apart from FITC, glutaraldehyde has been utilized to modify Lzm-AuNCs and aggregate red-emitting AuNCs into green-emitting Lzm-AuNPs through the conformation of C = N bonds [138]. While the pH changed slightly from 7.5 to 9.5, the green fluorescence of Lzm-AuNPs was increase but the red fluorescence of Lzm-AuNCs remained unchanged. The ratiometric probe has been applied to monitor pH change in dexamethasone-treated HeLa cells. In addition, another nanoprobe has been developed through self-assembly of GSH-AuNCs and using FITC-functionalized HA for ratiometric sensing and bioimaging of highly reactive oxygen species (hROS) [139]. Fluorescent AuNCs were also tried to in situ encapsule into zeolite imidazolate frameworks-8 (ZIF-8) to construct as nanosensors for ratiometric fluorescence sensing of acetylcholinesterase [140].

Disease therapy

Cancer therapy

Fluorescent AuNCs capped with biomolecules are promising nanomaterials for targeted cancer therapy via radiotherapy, photodynamic therapy (PDT), photothermal therapy (PTT) and combination therapy. BSA-AuNCs have been explored

as radiosensitizers [141, 142]. For example, Ghahremani et al. [143] have combined BSA-AuNCs with an antiproliferative oligonucleotide (AS1411 aptamer), widely used as a tumor-targeting agent. The combination of BSA-AuNCs and AS1411 aptamer exhibited good tumor cell targeting ability and improved efficacy of radiation therapy. Ultrasmall fluorescent GSH-AuNCs (~2 nm) have been widely investigated to be applied as radiosensitizers for radiation therapy. These untrasmall AuNCs could readily penetrate tumor tissue and move in blood vessels. Moreover, the low lymphatic outflow from tumor tissue made GSH-AuNCs less susceptible to clearance [106, 144]. GSH-AuNCs with EPR effect, could accumulate in tumors and show a strong radiosensitizing effect on cancer radiotherapy. They also had effective renal clearance and excellent biocompatibility in vivo. In addition, histidine-functionalized AuNCs have been developed for radiosensitizer with sensitization rate up to ~1.54 (Fig. 11A) [145]. Other fluorescent AuNCs functionalized targeting peptides and oligonucleotide aptamers have also been explored as radiosensitizers to enhance the cancer radiotherapy effects [146, 147]. These studies indicated that fluorescent bioligands-modified AuNCs are becoming one the most promising radiosensitizers for cancer therapy.

Photodynamic therapy (PDT) is approved a noninvasive therapeutic technique for cancer and other diseases treatments. It contains two separate nontoxic components: photosensitizers (PSs) and specific wavelengths of light to activate the PSs [148]. AuNCs modified with biomolecules have been applied as effective photosensitizers for imaging-guided PDT. For example, multifunctional AuNCs co-modified with human serum albumin (HSA) and catalase (CAT) have been developed as a multifunctional, therapeutic, diagnostic nano-agents [149]. The HSA-CAT-AuNCs produced singlet oxygen under a laser excitation (1064 nm), which exactly located in the NIR-II window, enabling NIR-II-triggered PDT. Compared to the conventional visible light-triggered PDT, NIR-II-induced PDT exhibited increased tissue penetration due to the low tissue absorption and scattering. This study indicated the HSA-CAT-AuNCs could act as a photosensitizing nano-agent for in vivo fluorescence imaging, tumor hypoxia relief, and NIR-II-triggered in vivo PDT in the treatment of cancer. BSA-AuNCs have been also employed as photosensitizers to improve PDT. Fluorescent AuNCs encapsulated into BSA nanospheres exhibited enhanced PDT effect, which had good cellular uptake, high $^1O_2$ production and excellent biocompatibility [150]. Dan et al. [151] have prepared novel BSA-AuNCs as photosensitizers with NIR-II fluorescence and peroxide-like activity, which possessed oxygen self-supply ability to enhance PDT. The study further demonstrated the BSA-AuNCs with enhanced PDT could be applied for cancer and bacterial infection treatments (Fig. 11B).

AuNCs functionalized with biomolecules have also been developed PTT, which relied on a photothermal transducer (PTA) to generate sufficient heat under NIR light irradiation for tumor inhibition or ablation [152]. $Au_{25}(SG)_{18}$ NCs have been synthesized and applied for PTT study of breast cancer cells. The NCs displayed good photothermal activity under 10 W cm^{-2} power irradiation and the cell death would reach up to 100% under the 10 W cm^{-2} power irradiation as 808 nm laser source. In addition, novel BSA-AuNCs and GSH-AuNCs nanomaterials have been introduced for PTT of tumors [153, 154]. Due to the complicated nature of tumor tissue, it is often difficult to eradicate the tumor thoroughly with a single treatment modality.

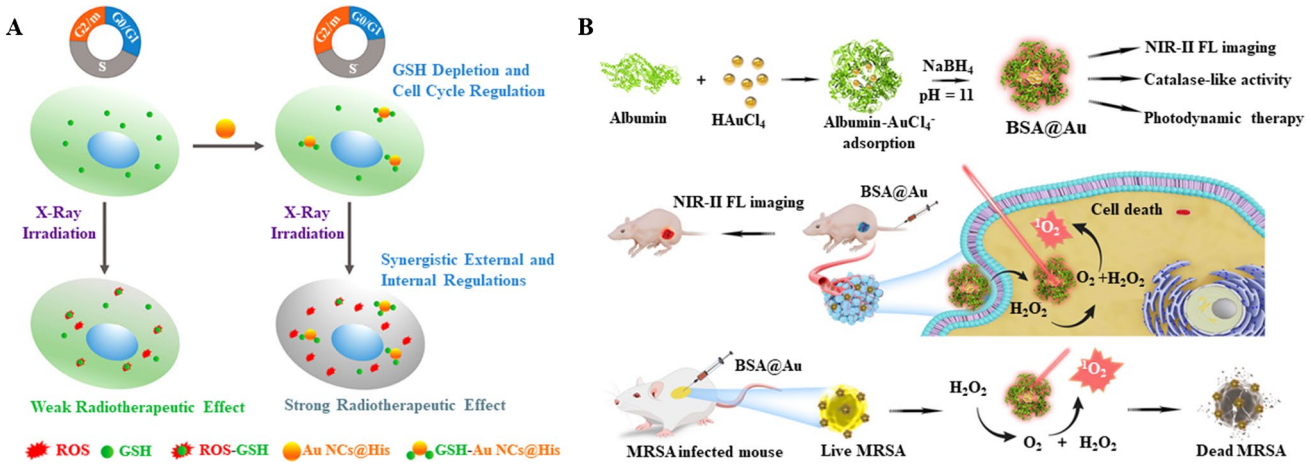

Fig. 11 (**A**) Schematic illustration of the therapeutic principle based on histidine-functionalized AuNCs for simultaneously increasing ROS generation, depleting GSH and regulating cell cycle. Reprinted with permission from Ref. [145]. Copyright 2018, American Chemical Society. (**B**) Schematic illustration of synthesis of NIR-II BSA-AuNCs combining with PDT against breast cancer and methicillin-resistant Staphylococcus aureus (MRSA) infection. Reprinted with permission from Ref. [151]. Copyright 2022, Qing Dan et al. Published by MDPI

Therefore, the integration of different treatment modalities is promising for tumor therapy. Currently, biomolecule-functionalized AuNCs-related PDT/PTT combination therapies, PTT/acoustic-photodynamic combination therapies, and photo-controlled PDT/PTT/chemotherapy combination therapies have also been investigated [155–158].

Antibacterial agents

Some of biomolecule-functionalized AuNCs, exhibiting high catalytic activity to generate ROS, can be applied as antibacterial agents to kill bacteria or microbial. Zheng et al. [159] have developed AuNPs protected with the ligand of 6-mercaptohexanoic acid (MHA) via precisely adjusting their size in the nanoclusters range. The resulted ultrasmall AuNCs exhibited efficient wide-spectrum antimicrobial activity, and the capability of killing both gram-positive and gram-negative bacteria via intracellular ROS induced by AuNCs [160]. Many other biomolecules are also introduced for the synthesis of AuNCs with antibacterial ability. Cys-protected AuNCs have been fabricated with orange-red-emitting fluorescence, high aqueous solubility and excellent biocompatibility [39] (Fig. 12A). The fluorescence intensity of Cys-AuNCs decreased in the presence of E. coli and the metabolism of Cys-AuNCs by E. coli accelerated the generation of intracellular ROS to kill E. coli. It suggested that Cys-AuNCs could be applied for bacterial detection and antimicrobial agents. Xie et al. [158] have synthesized deoxyribonuclease (DNase)-functionalized AuNCs, which killed the gram-positive and gram-negative bacteria (Fig. 12B). The extracellular polymeric substance matrix was decomposed by DNase and then the defenseless bacteria were exposed to PTT and PDT by DNase-AuNCs under 808 nm laser irradiation. ~ 90% Bacteria were killed in the process. In contrast to general belief that anionic nanoparticles were more likely to kill bacteria since it had positively charged cell wall, Li and coworkers [161] have constructed cationic AuAgNCs@BSA that could induce severe disruption of outer membrane metabolism due to strong electrostatic interactions and increase ROS accumulation leading bacteria to demise (Fig. 12C). It demonstrated that luminescent biomolecule-protected AuNCs had great potential for antimicrobial agents. In addition, novel AuNCs functionalized with quaternary ammonium (QA) salts have also been developed for antibiotic agent targeting multidrug-positive bacteria both in vitro and in vivo [32] (Fig. 12D).

Biocatalysis

The conventional biocatalysts are natural enzymes with capability of catalyzing chemical and biochemical reactions

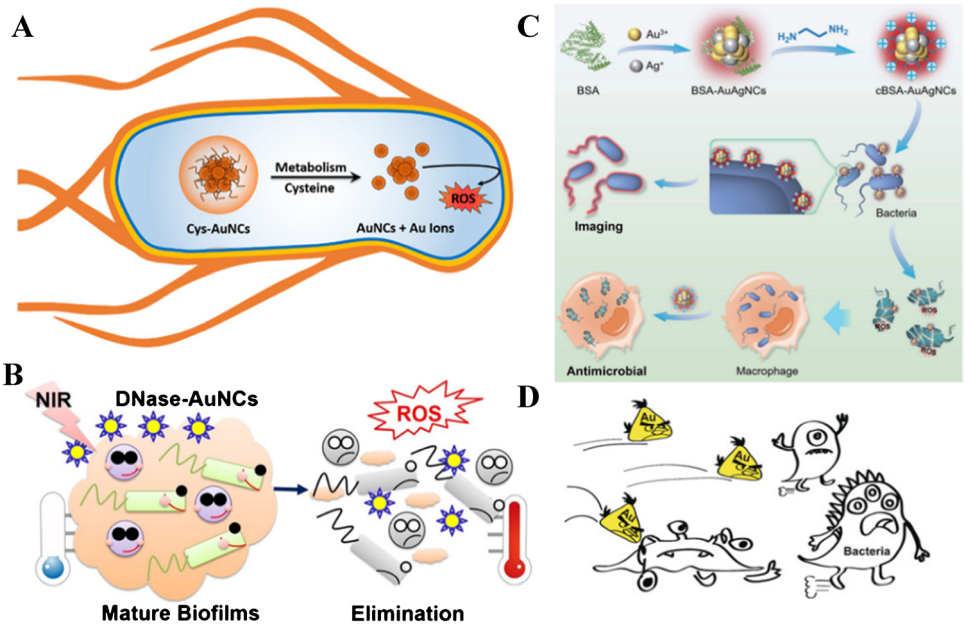

Fig. 12 (**A**) Schematic illustration of the mechanism of Cys-AuNCs killing E. coli. Reprinted with permission from Ref. [39]. Copyright 2019, American Chemical Society. (**B**) Schematic illustration of the cooperation of DNase-AuNCs with PTT and PDT to damage bacteria. Reprinted with permission from Ref. [158]. Copyright 2020, American Chemical Society. (**C**) Schematic illustration of the synthesis of cationic AuAgNCs@BSA and their applications in bioimaging and antibacterial agents. Reprinted with permission from Ref. [161]. Copyright 2022, Tsinghua University Press. (**D**) Schematic illustration of QA-AuNCs targeting multidrug-resistant bacteria. Reprinted with permission from Ref. [32]. Copyright 2018, Wiley–VCH

with superior catalytic activity and high substrate specificity. However, these natural enzymes are highly sensitive to environmental changes and can be readily denatured by stringent conditions. Mimetic enzymes have been widely developed with aims to obtain artificial biocatalysts with the advantages of easy and low-cost preparation, long-term stability, and tunable catalytic activity [162–164]. Among the investigated artificial enzymes, biomolecule-functionalized AuNCs have attracted particular attention [165]. Various nanozyme-like AuNCs have been developed and exhibited the POD-like, superoxide dismutase (SOD)-like, glucose oxidase-like, catalase (CAT)-like, protease-like, and nuclease-like activities, which can be used for biocatalysis and therapy.

BSA-modified AuNCs show prominent intrinsic POD-like activity [166]. BSA-AuNCs with nanozyme activity have been applied to catalyze the oxidation of a typical peroxidase substrate TMB in the presence of H_2O_2 to generate a blue-colored, oxidized substance (oxTMB). Due to the intrinsic POD-like activity, BSA-AuNCs have been used as sensitive and selective colorimetric sensors or probes for biological applications [167, 168]. For example, Tao et al. [169] have applied a robust biosensor based on the prominent artificial POD activity of BSA-AuNCs-loaded liposomes for the colorimetric detection of human epidermal growth factor receptor 2 (HER 2). Another BSA-capped AuNCs were developed and exhibited photo-stimulated POD-like activity upon irradiating with visible light in a reaction without H_2O_2. Due to the photo-stimulated artificial enzyme activity, the BSA-capped AuNCs can be used as biocompatible nanozymes for subsequent applications in bioimaging and biosensing [170].

SOD, as a metal holoenzyme and widely existing in plants, animals and microbes, can convert superoxide anions into hydrogen peroxide and oxygen, which then are converted to water by other enzymes. In recent years, mimetic enzymes with SOD-like activity, especially gold nanomaterials-based enzymes, have been widely designed and created because they can remove excess ROS and maintain the stability of the body, which are used in biomedicine, clinical and other fields [171, 172]. For the SOD catalytic process, it proposed that the Au nanozymes can adsorb $O_2\cdot^-$ or $HO_2\cdot$ and transfer their electrons to Au nanozymes, and then to catalyze the denaturation of $O_2\cdot^-$. Meanwhile, the Au cores have the electron storage capacity, acting as an electron reservoir [173, 174]. Red luminescent gold nanoclusters (CS-GSH-AuNCs) have been fabricated in HeLa cells using GSH as a template and cationic polymeric chitosan (CS) as crosslinker and stabilizer. The in situ synthesized CS-GSH-AuNCs had both SOD- and POD-like activities, which accelerated $O_2\cdot^-$ to form H_2O_2 and then ·OH. The enzyme-like activity of the AuNCs was effectively activated under acidic conditions, and exhibited an excellent killing effect on tumor cells but with low toxicity to normal cells (Fig. 13A) [175].

Multifunctional gold clusterzymes (LC-AuNCs) co-incorporated with lysozyme and curcumin (LC) have been synthesized, showing glucose oxidase-like activity and ROS-clearing capacity [33], which enabled the efficient removal excess glucose without producing additional H_2O_2, thereby alleviating the oxidative stress. In this work, LC-AuNCs-incorporated hydrogels was subsequently fabricated, acting as multifunctional dressings for regulating the regeneration cascade and promoting the healing of infected diabetic wound in vivo (Fig. 13B). Besides, Au nanomaterials with glucose oxidase-like activity have also been designed and fabricated for the detection of different analytes such as glucose. The mechanism investigation

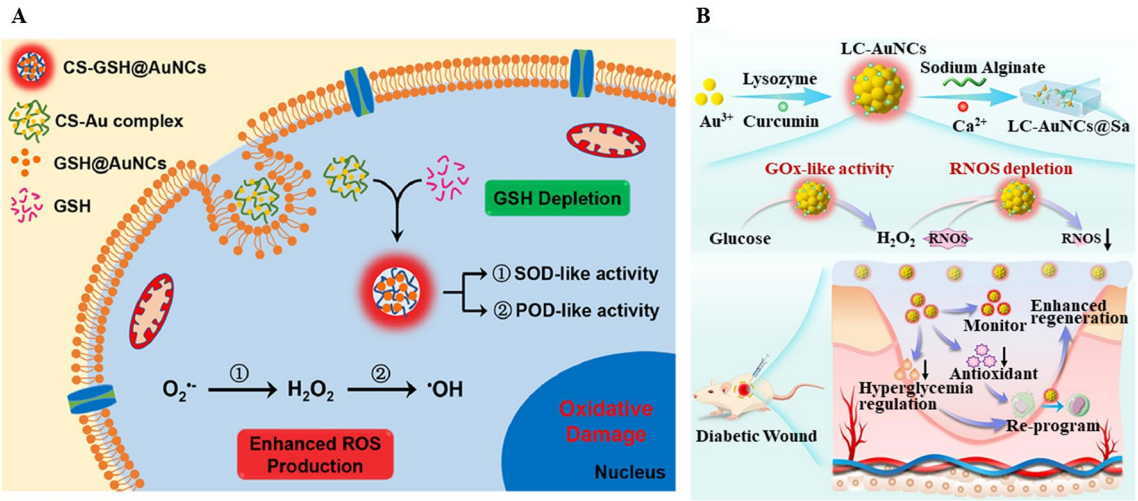

Fig. 13 (**A**) Schematic illustration of the in situ synthesized CS-GSH-AuNCs exhibit both SOD and POD-like activities in the nucleus. Reprinted with permission from Ref. [175]. Copyright 2021, Elsevier B.V. (**B**) Schematic illustration of the synthesis of LC-AuNCs and their application in diabetic wound healing. Reprinted with permission from Ref. [33]. Copyright 2024, Elsevier B.V

indicated that in the catalytic process, glucose and O_2 could co-adsorb onto the surface of AuNCs, which would promote two H atoms transfer to O_2 from glucose to H_2O_2, and then complete the catalytic cycle [176].

Catalase (CAT)-like nanozyme, regarding as an essential part of the regulation of ROS, has attracted great attention in recent years. AuNCs have been demonstrated to possess multifarious intrinsic enzyme properties including CAT-like activity [177]. Amine-terminated PAMAM dendrimer-entrapped AuNCs have been prepared, exhibiting POD-like activity and CAT-like activity. It demonstrated that the CAT-like activity still remained in physiological conditions while the POD-like activity would be lost in the same conditions [178]. In addition to the aforementioned enzyme-like activities, biomolecule-protected AuNCs with other enzymatic activities have also been investigated, such as protease-like [179], nuclease-like [180] and hydrolase enzyme-like activity [181], etc. Besides, the active AuNCs with enzyme-like activity can be developed other biomedical applications. For example, catalytically-active AuNCs with atomic precision have been fabricated for noninvasive early intervention of neurotrauma [182]. The AuNCs alleviated the oxidative stress and decreased the excessive $O_2{\cdot}^-$ and H_2O_2 in vitro and in vivo. They could also promote the wound healing of brain trauma and relieve inflammation through inhibiting the activation of astrocytes and microglia via noninvasive administration to decrease $O_2{\cdot}^-$ and H_2O_2 in brain tissue. In addition, a novel nano-platform (BGN-AuNCs) based on the supercharged AuNCs with enhanced enzyme-mimic activity as interface modulator of bioactive glass nanoparticles (BGN) has been constructed for infected wound treatment [183]. The supercharged AuNCs, showing strong affinity to BGN, would functionalize onto BGN and result in the robust immobilization of AuNCs on BGN. The AuNCs-functionalized BGN exhibited superior POD-like activity for catalytic antibacterial action.

In recent decades, fluorescent biomolecule-templated AuNCs have been widely synthesized via a variety of different approaches and these nanomaterials have drawn great attention in various biological applications. Apart from the above-mentioned applications in bioimaging, biosensing, cancer therapy, antibacterial agents and biocatalysis (especially nanozymes), they can also be applied for drug delivery [23]. Drug-loaded AuNCs have shown enhanced tumor penetrability and accumulation due to the EPR effect.

Conclusion and outlook

Biomolecule-templated AuNCs have been extensively investigated in the past decades due to their unique properties: ultrasmall size, large Stoke shifts, high fluorescence, good photostability, excellent biocompatibility as well as tunable emissions via bioligand modifications. A variety of biomolecules including amino acids, peptides, proteins and DNA have been developed for the functionalization of AuNCs for biological applications. They are widely used as bioimaging probes, biocatalysts and biosensors for detection of metal ions, small molecules, peptides and proteins. Also, they can be applied for cancer therapy, antibacterial agents, and nanomedicine applications.

Recent studies suggest the great progress on the synthetic strategies and the biological applications of fluorescent AuNCs. However, there are still challenges for the biomolecule-protected fluorescent AuNCs. Firstly, new synthetic approaches should be continuously exploited to prepare atomically precise AuNCs, and new ligands with some universality and controlled reduction can be created to help control the fabrication of AuNCs and stabilize AuNCs. Secondly, the precise structure of bioligand-stabilized AuNCs remains unclear and more advanced characterization techniques can be introduced to identify the structure. The development of efficient strategies for the purification of bio-templated AuNCs is beneficial for the identification of their precise structure. Thirdly, the toxicity, metabolic kinetics and mechanism of fluorescent AuNCs in living organisms require to be further studied and clarified. In addition, for the cancer therapy, more new protocols with combination of multi-therapies can be further developed to improve the efficacy of tumor therapy. Also, more different drug can be tried to load onto AuNCs to expand their nanomedicine applications. Moreover, to advance their applications, the aforementioned limitations of biomolecule-protected AuNCs due to their relatively weak luminescence and low quantum yield should be addressed. Currently, certain efficient strategies have been proposed and developed to prepare ultrabright biomolecule-protected AuNCs: 1) developing AuNCs-based composites by integrating with other functional motifs [184]; 2) using templates containing electron-rich elements [185, 186]; 3) increasing the electro-positivity of the Au core [53]; 4) functionalizing the surface ligands of AuNCs to restrict the intramolecular motion [187].

Acknowledgements The present study was funded by the National Natural Science Foundation of China (grant nos. 22274100 and 2223000319).

Author contribution Conceptualization, J.Q. and T.S.; methodology, J.M. and L.X.; software, Y.S. and Y.L.; validation, Y.L., Y.X. and L.X.; formal analysis, F.A.; investigation, J.Q. and Y.X.; resources, J.Q.; writing-original draft preparation, J.Q. and Y.X.; writing-review and editing, F.A., Y.X. and T.S.; supervision, T.S. and X.Z.; project administration, T.S; funding acquisition, T.S. and X.Z. All authors have read and agreed to the published version of the manuscript.

Declarations

Conflict of interest The authors have no conflicts of interest to declare.

References

1. Yau SH, Varnavski O, Goodson T III. An ultrafast look at Au nanoclusters. Acc Chem Res. 2013;46(7):1506–16.
2. Yahia-Ammar A, Sierra D, Mérola F, Hildebrandt N, Le Guével X. Self-assembled gold nanoclusters for bright fluorescence imaging and enhanced drug delivery. ACS Nano. 2016;10(2):2591–9.
3. Whetten RL, Weissker H-C, Pelayo JJ, Mullins SM, López-Lozano X, Garzón IL. Chiral-icosahedral (I) symmetry in ubiquitous metallic cluster compounds (145A, 60X): structure and bonding principles. Acc Chem Res. 2019;52(1):34–43.
4. Zhou M, Du X, Wang H, Jin R. The critical number of gold atoms for a metallic state nanocluster: resolving a decades-long question. ACS Nano. 2021;15(9):13980–92.
5. Chen L-Y, Wang C-W, Yuan Z, Chang H-T. Fluorescent gold nanoclusters: recent advances in sensing and imaging. Anal Chem. 2015;87(1):216–29.
6. Halawa M, Lai J, Xu G. Gold nanoclusters: synthetic strategies and recent advances in fluorescent sensing. Mater Today Nano. 2018;3:9–27.
7. Palmal S, Jana NR. Gold nanoclusters with enhanced tunable fluorescence as bioimaging probes. Wires Nanomed Nanobi. 2014;6(1):102–10.
8. Zhang KY, Yu Q, Wei H, Liu S, Zhao Q, Huang W. Long-lived emissive probes for time-resolved photoluminescence bioimaging and biosensing. Chem Rev. 2018;118(4):1770–839.
9. Chen W, Chen S. Oxygen electroreduction catalyzed by gold nanoclusters: strong core size effects. Angew Chem. 2009;121(24):4450–3.
10. Li G, Abroshan H, Liu C, Zhuo S, Li Z, Xie Y, et al. Tailoring the electronic and catalytic properties of Au_{25} nanoclusters via ligand engineering. ACS Nano. 2016;10(8):7998–8005.
11. Du Y, Sheng H, Astruc D, Zhu M. Atomically precise noble metal nanoclusters as efficient catalysts: a bridge between structure and properties. Chem Rev. 2019;120(2):526–622.
12. Shang L, Stockmar F, Azadfar N, Nienhaus GU. Intracellular thermometry by using fluorescent gold nanoclusters. Angew Chem Int Ed. 2013;52(42):11154–7.
13. Zheng Y, Lai L, Liu W, Jiang H, Wang X. Recent advances in biomedical applications of fluorescent gold nanoclusters. Adv Colloid Interfac. 2017;242:1–16.
14. Kailasa SK, Borse S, Koduru JR, Murthy Z. Biomolecules as promising ligands in the synthesis of metal nanoclusters: Sensing, bioimaging and catalytic applications. Trends Environ Anal. 2021;32:e00140.
15. Chen L, Gharib M, Zeng Y, Roy S, Nandi CK, Chakraborty I. Advances in bovine serum albumin-protected gold nanoclusters: from understanding the formation mechanisms to biological applications. Mater Today Chem. 2023;29:101460.
16. Shichibu Y, Negishi Y, Tsunoyama H, Kanehara M, Teranishi T, Tsukuda T. Extremely high stability of glutathionate-protected Au_{25} clusters against core etching. Small. 2007;3(5):835–9.
17. Deng H-H, Shi X-Q, Wang F-F, Peng H-P, Liu A-L, Xia X-H, et al. Fabrication of water-soluble, green-emitting gold nanoclusters with a 65% photoluminescence quantum yield via host–guest recognition. Chem Mater. 2017;29(3):1362–9.
18. Zheng K, Setyawati MI, Leong DT, Xie J. Surface ligand chemistry of gold nanoclusters determines their antimicrobial ability. Chem Mater. 2018;30(8):2800–8.
19. Pensa E, Azofra LM, Salvarezza RC, Carro P. Effect of ligands on the stability of gold nanoclusters. J Phys Chem Lett. 2022;13(28):6475–80.
20. Xie J, Zheng Y, Ying JY. Protein-directed synthesis of highly fluorescent gold nanoclusters. J Am Chem Soc. 2009;131(3):888–9.
21. Srinivasulu YG, Yao Q, Goswami N, Xie J. Interfacial engineering of gold nanoclusters for biomedical applications. Mater Horiz. 2020;7(10):2596–618.
22. Yang G, Wang Z, Du F, Jiang F, Yuan X, Ying JY. Ultrasmall coinage metal nanoclusters as promising theranostic probes for biomedical applications. J Am Chem Soc. 2023;145(22):11879–98.
23. Ding C, Xu Y, Zhao Y, Zhong H, Luo X. Fabrication of BSA@AuNC-based nanostructures for cell fluoresce imaging and target drug delivery. ACS Appl Mater Interfaces. 2018;10(10):8947–54.
24. Zhang Y, Wu M, Dai W, Chen M, Guo Z, Wang X, et al. High drug-loading gold nanoclusters for responsive glucose control in type 1 diabetes. J Nanobiotechnol. 2019;17(1):1–11.
25. Li Y, Zheng H, Lu H, Duan M, Li C, Li M, et al. Noncanonical condensation of nucleic acid chains by hydrophobic gold nanocrystals. J Am Chem Soc Au. 2023;3(8):2206–15.
26. Farkhani SM, Dehghankelishadi P, Refaat A, Gopal DV, Cifuentes-Rius A, Voelcker NH. Tailoring gold nanocluster properties for biomedical applications: from sensing to bioimaging and theranostics. Prog Mater Sci. 2023;142:101229. https://doi.org/10.1016/j.pmatsci.2023.101229
27. Zhang S, Zhang X, Su Z. Biomolecule conjugated metal nanoclusters: bio-inspiration strategies, targeted therapeutics, and diagnostics. J Mater Chem B. 2020;8(19):4176–94.
28. Cui H, Shao Z-S, Song Z, Wang Y-B, Wang H-S. Development of gold nanoclusters: from preparation to applications in the field of biomedicine. J Mater Chem C. 2020;8(41):14312–33.
29. Hao D, Zhang X, Su R, Wang Y, Qi W. Biomolecule-protected gold nanoclusters: synthesis and biomedical applications. J Mater Chem B. 2023;11(23):5051–70.
30. Li W, Zhou X, Yan W, Wang R, Yang Z, Hu Y, et al. Lysozyme-encapsulated gold nanoclusters for ultrasensitive detection of folic acid and in vivo imaging. Talanta. 2023;251:123789.
31. Yu F, Xiang H, He S, Zhao G, Cao Z, Yang L, et al. Gold nanocluster-based ratiometric fluorescent probe for biosensing of Hg^{2+} ions in living organisms. Analyst. 2022;147(12):2773–8.
32. Xie Y, Liu Y, Yang J, Liu Y, Hu F, Zhu K, et al. Gold nanoclusters for targeting methicillin-resistant staphylococcus aureus in vivo. Angew Chem Int Edit. 2018;57(15):3958–62.
33. Wang T, Xu Z, Wen M, Li N, Zhang L, Xue Y, et al. Multifunctional gold clusterzymes with distinct glucose depletion and macrophage reprogramming capability towards regulating the regeneration cascade. Chem Eng J. 2024;482:149068.
34. Jiao T, Yan X, Balan L, Stepanov AL, Chen X, Hu MZ. Chemical functionalization, self-assembly, and applications of nanomaterials and nanocomposites. J Nanomater. 2014;2014:2–2.
35. Dai Z, Tan Y, He K, Chen H, Liu J. Strict DNA valence control in ultrasmall thiolate-protected near-infrared-emitting gold nanoparticles. J Am Chem Soc. 2020;142(33):14023–7.
36. Yang L, Chen J, Huang T, Huang L, Sun Z, Jiang Y, et al. Red-emitting Au_7 nanoclusters with fluorescence sensitivity to Fe^{2+} ions. J Mater Chem C. 2017;5(18):4448–54.
37. Bain D, Maity S, Debnath T, Das AK, Patra A. Luminescent Au_6 and Au_8 nanoclusters from ligand induced etching of Au nanoparticles. Mater Res Express. 2019;6(12):124004.
38. Wu G. Amino acids: metabolism, functions, and nutrition. Amino Acids. 2009;37:1–17.
39. Chang T-K, Cheng T-M, Chu H-L, Tan S-H, Kuo J-C, Hsu P-H, et al. Metabolic mechanism investigation of antibacterial active cysteine-conjugated gold nanoclusters in Escherichia coli. ACS Sustainable Chem Eng. 2019;7(18):15479–86.
40. Jin R, Qian H, Wu Z, Zhu Y, Zhu M, Mohanty A, et al. Size focusing: a methodology for synthesizing atomically precise gold nanoclusters. J Phys Chem Lett. 2010;1(19):2903–10.
41. Xu S, Yang H, Zhao K, Li J, Mei L, Xie Y, et al. Simple and rapid preparation of orange-yellow fluorescent gold

nanoclusters using DL-homocysteine as a reducing/stabilizing reagent and their application in cancer cell imaging. Rsc Adv. 2015;5(15):11343–8.
42. Abarghoei S, Fakhri N, Borghei YS, Hosseini M, Ganjali MR. A colorimetric paper sensor for citrate as biomarker for early stage detection of prostate cancer based on peroxidase-like activity of cysteine-capped gold nanoclusters. Spectrochim Acta A. 2019;210:251–9.
43. Peng Y, Wang M, Wu X, Wang F, Liu L. Methionine-capped gold nanoclusters as a fluorescence-enhanced probe for cadmium (II) sensing. Sensors. 2018;18(2):658.
44. Yang X, Shi M, Zhou R, Chen X, Chen H. Blending of $HAuCl_4$ and histidine in aqueous solution: a simple approach to the Au_{10} cluster. Nanoscale. 2011;3(6):2596–601.
45. Zheng S, Yin H, Li Y, Bi F, Gan F. One–step synthesis of L-tryptophan-stabilized dual-emission fluorescent gold nanoclusters and its application for Fe^{3+} sensing. Sensor Actuat B-Chem. 2017;242:469–75.
46. Basu S, Paul A, Chattopadhyay A. Zinc mediated crystalline assembly of gold nanoclusters for expedient hydrogen storage and sensing. J Mater Chem A. 2016;4(4):1218–23.
47. Xu Y, Yang X, Zhu S, Dou Y. Selectively fluorescent sensing of Cu^{2+} based on lysine-functionalized gold nanoclusters. Colloid Surface A. 2014;450:115–20.
48. Fu W, Wang H, Chen Y, Ding J, Shan G. Fluorescence sensing analysis for rapid detection of serum glutathione based on degrading AuNCs@Lys-MnO_2 fluorescence resonance energy transfer system. Microchem J. 2020;159:105556.
49. Mu X, Qi L, Dong P, Qiao J, Hou J, Nie Z, et al. Facile one-pot synthesis of L-proline-stabilized fluorescent gold nanoclusters and its application as sensing probes for serum iron. Biosens Bioelectron. 2013;49:249–55.
50. Yang X, Luo Y, Zhuo Y, Feng Y, Zhu S. Novel synthesis of gold nanoclusters templated with L-tyrosine for selective analyzing tyrosinase. Anal Chim Acta. 2014;840:87–92.
51. Borsook H. Peptide bond formation. Adv Protein Chem. 1953;8:127–74.
52. Fabris L, Antonello S, Armelao L, Donkers RL, Polo F, Toniolo C, et al. Gold nanoclusters protected by conformationally constrained peptides. J Am Chem Soc. 2006;128(1):326–36.
53. Wu Z, Jin R. On the ligand's role in the fluorescence of gold nanoclusters. Nano Lett. 2010;10(7):2568–73.
54. Radenković S, Antić M, Savić ND, Glišić BĐ. The nature of the Au–N bond in gold (III) complexes with aromatic nitrogen-containing heterocycles: The influence of Au (III) ions on the ligand aromaticity. New J Chem. 2017;41(21):12407–15.
55. An D, Su J, Weber JK, Gao X, Zhou R, Li J. A peptide-coated gold nanocluster exhibits unique behavior in protein activity inhibition. J Am Chem Soc. 2015;137(26):8412–8.
56. Wu Z, Suhan J, Jin R. One-pot synthesis of atomically monodisperse, thiol-functionalized Au_{25} nanoclusters. J Mater Chem. 2009;19(5):622–6.
57. Luo Z, Yuan X, Yu Y, Zhang Q, Leong DT, Lee JY, et al. From aggregation-induced emission of Au (I)–thiolate complexes to ultrabright Au(0)@Au(I)–thiolate core–shell nanoclusters. J Am Chem Soc. 2012;134(40):16662–70.
58. Wu Z, Wang M, Yang J, Zheng X, Cai W, Meng G, et al. Well-defined nanoclusters as fluorescent nanosensors: a case study on $Au_{25}(SG)_{18}$. Small. 2012;8(13):2028–35.
59. Zhao R-X, Liu A-Y, Wen Q-L, Wu B-C, Wang J, Hu Y-L, et al. Glutathione stabilized green-emission gold nanoclusters for selective detection of cobalt ion. Spectrochimica Acta A. 2021;254:119628.
60. You J-G, Tseng W-L. Peptide-induced aggregation of glutathione-capped gold nanoclusters: a new strategy for designing aggregation-induced enhanced emission probes. Anal Chim Acta. 2019;1078:101–11.
61. Cao L, Chen W-Q, Zhou L-J, Wang Y-Y, Liu Y, Jiang F-L. Regulation of the enzymatic activities of lysozyme by the surface ligands of ultrasmall gold nanoclusters: the role of hydrophobic interactions. Langmuir. 2021;37(46):13787–97.
62. Pranantyo D, Liu P, Zhong W, Kang E-T, Chan-Park MB. Antimicrobial peptide-reduced gold nanoclusters with charge-reversal moieties for bacterial targeting and imaging. Biomacromol. 2019;20(8):2922–33.
63. Wang Y, Cui Y, Zhao Y, Liu R, Sun Z, Li W, et al. Bifunctional peptides that precisely biomineralize Au clusters and specifically stain cell nuclei. Chem Commun. 2012;48(6):871–3.
64. Song W, Wang Y, Liang R-P, Zhang L, Qiu J-D. Label-free fluorescence assay for protein kinase based on peptide biomineralized gold nanoclusters as signal sensing probe. Biosens Bioelectron. 2015;64:234–40.
65. Tao Y, Zhang Y, Ju E, Ren H, Ren J. Gold nanocluster-based vaccines for dual-delivery of antigens and immunostimulatory oligonucleotides. Nanoscale. 2015;7(29):12419–266.
66. Wang Y, Cui Y, Liu R, Gao F, Gao L, Gao X. Bio-inspired peptide-Au cluster applied for mercury (II) ions detection. Sci China Chem. 2015;58:819–24.
67. Liu S, Jia Y, Xue J, Li Y, Wu Z, Ren X, et al. Bifunctional peptide-biomineralized gold nanoclusters as electrochemiluminescence probe for optimizing sensing interface. Sensor Actuat B-Chem. 2020;318:128278.
68. Anfinsen CB. The formation and stabilization of protein structure. Biochem J. 1972;128(4):737.
69. Xu Y, Sherwood J, Qin Y, Crowley D, Bonizzoni M, Bao Y. The role of protein characteristics in the formation and fluorescence of Au nanoclusters. Nanoscale. 2014;6(3):1515–24.
70. Xie J, Zheng Y, Ying JY. Highly selective and ultrasensitive detection of Hg^{2+} based on fluorescence quenching of Au nanoclusters by Hg^{2+}–Au^{+} interactions. Chem Commun. 2010;46(6):961–3.
71. Zhang J, Zhang Z, Nie X, Zhang Z, Wu X, Chen C, et al. A label-free gold nanocluster fluorescent probe for protease activity monitoring. J Nanosci Nanotechno. 2014;14(6):4029–35.
72. Xavier PL, Chaudhari K, Verma PK, Pal SK, Pradeep T. Luminescent quantum clusters of gold in transferrin family protein, lactoferrin exhibiting FRET. Nanoscale. 2010;2(12):2769–76.
73. Li L, Lu Y, Xu X, Yang X, Chen L, Jiang C, et al. Catalytic-enhanced lactoferrin-functionalized Au-Bi_2Se_3 nanodots for Parkinson's disease therapy via reactive oxygen attenuation and mitochondrial protection. Adv Healthc Mater. 2021;10(13):2100316.
74. Shao C, Yuan B, Wang H, Zhou Q, Li Y, Guan Y, et al. Eggshell membrane as a multimodal solid state platform for generating fluorescent metal nanoclusters. J Mater Chem. 2011;21(9):2863–6.
75. Zhang P, Lan J, Wang Y, Huang CZ. Luminescent golden silk and fabric through in situ chemically coating pristine-silk with gold nanoclusters. Biomaterials. 2015;36:26–32.
76. Li Z, Peng H, Liu J, Tian Y, Yang W, Yao J, et al. Plant protein-directed synthesis of luminescent gold nanocluster hybrids for tumor imaging. ACS Appl Mater Interfaces. 2018;10(1):83–90.
77. Liu H, Gu T, Yu W, Xing Y, Zhou J. Observation of luminescent gold nanoclusters using one-step syntheses from wool keratin and silk fibroin effect. Eur Polym J. 2018;99:1–8.
78. Shu T, Cheng X, Wang J, Lin X, Zhou Z, Su L, et al. Synthesis of luminescent gold nanoclusters embedded goose feathers for facile preparation of Au (I) complexes with aggregation-induced emission. ACS Sustainable Chem Eng. 2018;7(1):592–8.
79. Cheng X, Shu T, Sun Y, Zhou X, An J, Dai Q, et al. "Gold inlaid with hair": permanent fluorescent hair dyeing using fast

protein-assisted biomineralization of gold nanoclusters. ACS Sustainable Chem Eng. 2021;10(1):305–13.
80. Carnerero JM, Jimenez-Ruiz A, Castillo PM, Prado-Gotor R. Covalent and non-covalent DNA–gold-nanoparticle interactions: new avenues of research. ChemPhysChem. 2017;18(1):17–33.
81. Koo KM, Sina AA, Carrascosa LG, Shiddiky MJ, Trau M. DNA–bare gold affinity interactions: mechanism and applications in biosensing. Anal Methods. 2015;7(17):7042–54.
82. Lopez A, Liu J. Light-activated metal-coordinated supramolecular complexes with charge-directed self-assembly. The J Phys Chem C. 2013;117(7):3653–61.
83. Nakamura T, Zhao Y, Yamagata Y, Hua Y-J, Yang W. Watching DNA polymerase η make a phosphodiester bond. Nature. 2012;487(7406):196–201.
84. Liu J. DNA-stabilized, fluorescent, metal nanoclusters for biosensor development. Trac-Trend Anal Chem. 2014;58:99–111.
85. Hosseini M, Ahmadi E, Borghei Y-S, Ganjali MR. A new fluorescence turn-on nanobiosensor for the detection of micro-RNA-21 based on a DNA–gold nanocluster. Methods Appl Fluores. 2017;5(1):015005.
86. Wang M, Chen Y, Cai W, Feng H, Du T, Liu W, et al. In situ self-assembling Au-DNA complexes for targeted cancer bioimaging and inhibition. P Natl A Sci. 2020;117(1):308–16.
87. Wang HB, Mao AL, Li YH, Gan T, Liu YM. A turn-on fluorescence strategy for biothiols determination by blocking Hg (II)-mediated fluorescence quenching of adenine-rich DNA-templated gold nanoclusters. Luminescence. 2020;35(8):1296–303.
88. Kryachko E, Remacle F. Complexes of DNA bases and gold clusters Au_3 and Au_4 involving nonconventional N− H…Au hydrogen bonding. Nano Lett. 2005;5(4):735–9.
89. Liu G, Shao Y, Ma K, Cui Q, Wu F, Xu S. Synthesis of DNA-templated fluorescent gold nanoclusters. Gold Bull. 2012;45:69–74.
90. Liu G, Shao Y, Wu F, Xu S, Peng J, Liu L. DNA-hosted fluorescent gold nanoclusters: sequence-dependent formation. Nanotechnology. 2012;24(1):015503.
91. Lopez A, Liu J. DNA-templated fluorescent gold nanoclusters reduced by Good's buffer: from blue-emitting seeds to red and near infrared emitters. Can J Chem. 2015;93(6):615–20.
92. Wang Y, Wang X, Ma X, Chen Q, He H, Nau WM, et al. Coassembly of gold nanoclusters with nucleic acids: sensing, bioimaging, and gene transfection. Part Part Syst Char. 2019;36(10):1900281.
93. Quan Z, Xue F, Li H, Chen Z, Wang L, Zhu H, et al. A bioinspired ratiometric fluorescence probe based on cellulose nanocrystal-stabilized gold nanoclusters for live-cell and zebrafish imaging of highly reactive oxygen species. Chem Eng J. 2022;431:133954.
94. Duan Y, Duan R, Liu R, Guan M, Chen W, Ma J, et al. Chitosan-stabilized self-assembled fluorescent gold nanoclusters for cell imaging and biodistribution in vivo. ACS Biomater Sci Eng. 2018;4(3):1055–63.
95. Chandirasekar S, Chandrasekaran C, Muthukumarasamyvel T, Sudhandiran G, Rajendiran N. Biosurfactant templated quantum sized fluorescent gold nanoclusters for in vivo bioimaging in zebrafish embryos. Colloids Surf B Biointerfaces. 2016;143:472–80.
96. Wang J-Q, He R-L, Liu W-D, Feng Q-Y, Zhang Y-E, Liu C-Y, et al. Integration of metal catalysis and organocatalysis in a metal nanocluster with anchored proline. J Am Chem Soc. 2023;145(22):12255–63.
97. Yuan Q, Wang Y, Zhao L, Liu R, Gao F, Gao L, et al. Peptide protected gold clusters: chemical synthesis and biomedical applications. Nanoscale. 2016;8(24):12095–104.
98. Zare I, Chevrier DM, Cifuentes-Rius A, Moradi N, Xianyu Y, Ghosh S, et al. Protein-protected metal nanoclusters as diagnostic and therapeutic platforms for biomedical applications. Mater Today. 2023;66:159–93.
99. Ding C, Tian Y. Gold nanocluster-based fluorescence biosensor for targeted imaging in cancer cells and ratiometric determination of intracellular pH. Biosens Bioelectron. 2015;65:183–90.
100. Hada A-M, Craciun A-M, Focsan M, Borlan R, Soritau O, Todea M, et al. Folic acid functionalized gold nanoclusters for enabling targeted fluorescence imaging of human ovarian cancer cells. Talanta. 2021;225:121960.
101. Retnakumari A, Setua S, Menon D, Ravindran P, Muhammed H, Pradeep T, et al. Molecular-receptor-specific, non-toxic, near-infrared-emitting Au cluster-protein nanoconjugates for targeted cancer imaging. Nanotechnology. 2009;21(5):055103.
102. Bhamore JR, Deshmukh B, Haran V, Jha S, Singhal RK, Lenka N, et al. One-step eco-friendly approach for the fabrication of synergistically engineered fluorescent copper nanoclusters: sensing of Hg^{2+} ion and cellular uptake and bioimaging properties. New J Chem. 2018;42(2):1510–20.
103. Bertorelle F, Wegner KD, Perić Bakulić M, Fakhouri H, Comby-Zerbino C, Sagar A, et al. Tailoring the NIR-II photoluminescence of single thiolated Au_{25} nanoclusters by selective binding to proteins. Chem–A Eur J. 2022;28(39):e202200570.
104. Zhang C, Gao X, Chen W, He M, Yu Y, Gao G, et al. Advances of gold nanoclusters for bioimaging. iScience. 2022;25(10):105022. https://doi.org/10.1016/j.isci.2022.105022
105. Sun Y, Wu J, Wang C, Zhao Y, Lin Q. Tunable near-infrared fluorescent gold nanoclusters: temperature sensor and targeted bioimaging. New J Chem. 2017;41(13):5412–9.
106. Liu H, Hong G, Luo Z, Chen J, Chang J, Gong M, et al. Atomic-precision gold clusters for NIR-II imaging. Adv Mater. 2019;31(46):1901015.
107. Li D, Liu Q, Qi Q, Shi H, Hsu EC, Chen W, et al. Gold nanoclusters for NIR-II fluorescence imaging of bones. Small. 2020;16(43):2003851.
108. Zhang C, Zhou Z, Qian Q, Gao G, Li C, Feng L, et al. Glutathione-capped fluorescent gold nanoclusters for dual-modal fluorescence/X-ray computed tomography imaging. J Mater Chem B. 2013;1(38):5045–53.
109. Zheng B, Wu Q, Jiang Y, Hou M, Zhang P, Liu M, et al. One-pot synthesis of ^{68}Ga-doped ultrasmall gold nanoclusters for PET/CT imaging of tumors. Mat Sci Eng C. 2021;128:112291.
110. He K, Yu S, Wang X, Li D, Chen J, Zhong H, et al. The fabrication of transferrin-modified two-photon gold nanoclusters with near-infrared fluorescence and their application in bioimaging. Chem Commun. 2021;57(80):10391–4.
111. Zhong W, Liang K, Liu W, Shang L. Ligand-protected nanocluster-mediated photoswitchable fluorescent nanoprobes towards dual-color cellular imaging. Chem Sci. 2023;14(33):8823–30.
112. Wu X, He X, Wang K, Xie C, Zhou B, Qing Z. Ultrasmall near-infrared gold nanoclusters for tumor fluorescence imaging in vivo. Nanoscale. 2010;2(10):2244–9.
113. Xu C, Wang Y, Zhang C, Jia Y, Luo Y, Gao X. AuGd integrated nanoprobes for optical/MRI/CT triple-modal in vivo tumor imaging. Nanoscale. 2017;9(13):4620–8.
114. Chen H, Li B, Ren X, Li S, Ma Y, Cui S, et al. Multifunctional near-infrared-emitting nano-conjugates based on gold clusters for tumor imaging and therapy. Biomaterials. 2012;33(33):8461–76.
115. Wang Y, Xu C, Zhai J, Gao F, Liu R, Gao L, et al. Label-free Au cluster used for in vivo 2D and 3D computed tomography of murine kidneys. Anal Chem. 2015;87(1):343–5.
116. Yang Z, Zhao Y, Hao Y, Li X, Zvyagin AV, Whittaker AK, et al. Ultrasmall red fluorescent gold nanoclusters for highly biocompatible and long-time nerve imaging. Part Part Syst Char. 2021;38(5):2100001.
117. Pang Z, Yan W, Yang J, Li Q, Guo Y, Zhou D, et al. Multifunctional gold nanoclusters for effective targeting, near-infrared fluorescence imaging, diagnosis, and treatment of cancer lymphatic metastasis. ACS Nano. 2022;16(10):16019–37.

118. Ni S, Liu Y, Tong S, Li S, Song X. Emerging NIR-II luminescent gold nanoclusters for in vivo bioimaging. J Anal Test. 2023;7(3):260–71.
119. Wang W, Kong Y, Jiang J, Xie Q, Huang Y, Li G, et al. Engineering the protein corona structure on gold nanoclusters enables red-shifted emissions in the second near-infrared window for gastrointestinal imaging. Angew Chem Int Edit. 2020;59(50):22431–5.
120. Yu X, Liu W, Deng X, Yan S, Su Z. Gold nanocluster embedded bovine serum albumin nanofibers-graphene hybrid membranes for the efficient detection and separation of mercury ion. Chem Eng J. 2018;335:176–84.
121. Qing T, Bu H, He X, He D, Zhou B, Sun H, et al. A selective nanosensor for ultrafast detection of Cu^{2+} ions based on C5 DNA-templated gold nanoclusters and Fenton-like reaction. Anal Methods. 2017;9(44):6222–7.
122. Shamsipur M, Babaee E, Gholivand M-B, Molaabasi F, Mousavi F, Barati A, et al. Bright green light-emitting gold nanoclusters confined in insulin as selective fluorescent switch probes for sensing and imaging of copper ions and glutathione. ACS Appl Nano Mater. 2023;6(7):5939–51.
123. Tian Y, Fuller E, Klug S, Lee F, Su F, Zhang L, et al. A fluorescent colorimetric pH sensor and the influences of matrices on sensing performances. Sensor Actuat B-Chem. 2013;188:1–10.
124. Xu H, Zhu H, Sun M, Yu H, Li H, Ma F, et al. Graphene oxide supported gold nanoclusters for the sensitive and selective detection of nitrite ions. Analyst. 2015;140(5):1678–85.
125. Liu J-M, Cui M-L, Jiang S-L, Wang X-X, Lin L-P, Jiao L, et al. BSA-protected gold nanoclusters as fluorescent sensor for selective and sensitive detection of pyrophosphate. Anal Methods. 2013;5(16):3942–7.
126. Wang C-W, Chen Y-N, Wu B-Y, Lee C-K, Chen Y-C, Huang Y-H, et al. Sensitive detection of cyanide using bovine serum albumin-stabilized cerium/gold nanoclusters. Anal Bioanal Chem. 2016;408:287–94.
127. Aswathy B, Sony G. Cu^{2+} modulated BSA–Au nanoclusters: a versatile fluorescence turn-on sensor for dopamine. Microchem J. 2014;116:151–6.
128. Mathew MS, Baksi A, Pradeep T, Joseph K. Choline-induced selective fluorescence quenching of acetylcholinesterase conjugated Au@BSA clusters. Biosens Bioelectron. 2016;81:68–74.
129. Hemmateenejad B, Shakerizadeh-shirazi F, Samari F. BSA-modified gold nanoclusters for sensing of folic acid. Sensor Actuat B-Chem. 2014;199:42–6.
130. Wang X, Wu P, Lv Y, Hou X. Ultrasensitive fluorescence detection of glutaraldehyde in water samples with bovine serum albumin-Au nanoclusters. Microchem J. 2011;99(2):327–31.
131. Chen X, Baker GA. Cholesterol determination using protein-templated fluorescent gold nanocluster probes. Analyst. 2013;138(24):7299–302.
132. Zhang X, Qiao J, Liu W, Qi L. Boosting the peroxidase-like activity of gold nanoclusters for the colorimetric detection of oxytetracycline in rat serum. Analyst. 2021;146(16):5061–6.
133. Tao Y, Ran X, Ren J, Qu X. Array-based sensing of proteins and bacteria by using multiple luminescent nanodots as fluorescent probes. Small. 2014;10(18):3667–71.
134. Zhao Y, Wang X, Mi J, Jiang Y, Wang C. Metal nanoclusters–based ratiometric fluorescent probes from design to sensing applications. Part Part Syst Char. 2019;36(11):1900298.
135. Santhoshkumar S, Madhu M, Tseng W-B, Tseng W-L. Gold nanocluster-based fluorescent sensors for in vitro and in vivo ratiometric imaging of biomolecules. Phys Chem Chem Phys. 2023;25(33):21787–801.
136. Tsai C-L, Chen J-C, Wang W-J. Near-infrared absorption property of biological soft tissue constituents. J Med Biol Eng. 2001;21(1):7–14.
137. Ke C-Y, Wu Y-T, Tseng W-L. Fluorescein-5-isothiocyanate-conjugated protein-directed synthesis of gold nanoclusters for fluorescent ratiometric sensing of an enzyme–substrate system. Biosens Bioelectron. 2015;69:46–53.
138. Chandirasekar S, You J-G, Xue J-H, Tseng W-L. Synthesis of gold nanocluster-loaded lysozyme nanoparticles for label-free ratiometric fluorescent pH sensing: applications to enzyme–substrate systems and cellular imaging. J Mater Chem B. 2019;7(24):3876–83.
139. Ran X, Wang Z, Pu F, Liu Z, Ren J, Qu X. Aggregation-induced emission-active Au nanoclusters for ratiometric sensing and bioimaging of highly reactive oxygen species. Chem Commun. 2019;55(100):15097–100.
140. Li Q, Zhou X, Tan L-L, Shang L. MOF-based surface tailoring the near-infrared luminescence property of gold nanoclusters for ratiometric fluorescence sensing of acetylcholinesterase. Sensor Actuat B-Chem. 2023;385:133695.
141. Barnett GC, West CM, Dunning AM, Elliott RM, Coles CE, Pharoah PD, et al. Normal tissue reactions to radiotherapy: towards tailoring treatment dose by genotype. Nat Rev Cancer. 2009;9(2):134–42.
142. Lord CJ, Ashworth A. The DNA damage response and cancer therapy. Nature. 2012;481(7381):287–94.
143. Ghahremani F, Shahbazi-Gahrouei D, Kefayat A, Motaghi H, Mehrgardi MA, Javanmard SH. AS1411 aptamer conjugated gold nanoclusters as a targeted radiosensitizer for megavoltage radiation therapy of 4T1 breast cancer cells. RSC Adv. 2018;8(8):4249–58.
144. Zhang XD, Luo Z, Chen J, Shen X, Song S, Sun Y, et al. Ultrasmall $Au_{10-12}(SG)_{10-12}$ nanomolecules for high tumor specificity and cancer radiotherapy. Adv Mater. 2014;26(26):4565–8.
145. Zhang X, Chen X, Jiang Y-W, Ma N, Xia L-Y, Cheng X, et al. Glutathione-depleting gold nanoclusters for enhanced cancer radiotherapy through synergistic external and internal regulations. ACS Appl Mater Interfaces. 2018;10(13):10601–6.
146. Fang X, Wang Y, Ma X, Li Y, Zhang Z, Xiao Z, et al. Mitochondria-targeting Au nanoclusters enhance radiosensitivity of cancer cells. J Mater Chem B. 2017;5(22):4190–7.
147. Luo D, Wang X, Zeng S, Ramamurthy G, Burda C, Basilion JP. Targeted gold nanocluster-enhanced radiotherapy of prostate cancer. Small. 2019;15(34):1900968.
148. Felsher DW. Cancer revoked: oncogenes as therapeutic targets. Nat Rev Cancer. 2003;3(5):375–9.
149. Chen Q, Chen J, Yang Z, Zhang L, Dong Z, Liu Z. NIR-II light activated photodynamic therapy with protein-capped gold nanoclusters. Nano Res. 2018;11:5657–69.
150. Geng T, Zhao L, Wu D, Zhang H, Zhao X, Jiao M, et al. Bovine serum albumin-encapsulated ultrasmall gold nanoclusters for photodynamic therapy of tumors. ACS Appl Nano Mater. 2021;4(12):13818–25.
151. Dan Q, Yuan Z, Zheng S, Ma H, Luo W, Zhang L, et al. Gold nanoclusters-based NIR-II photosensitizers with catalase-like activity for boosted photodynamic therapy. Pharmaceutics. 2022;14(8):1645.
152. Hu J-J, Cheng Y-J, Zhang X-Z. Recent advances in nanomaterials for enhanced photothermal therapy of tumors. Nanoscale. 2018;10(48):22657–72.
153. Gu W, Zhang Q, Zhang T, Li Y, Xiang J, Peng R, et al. Hybrid polymeric nano-capsules loaded with gold nanoclusters and indocyanine green for dual-modal imaging and photothermal therapy. J Mater Chem B. 2016;4(5):910–9.
154. Zhao P, Liu S, Wang L, Liu G, Cheng Y, Lin M, et al. Alginate mediated functional aggregation of gold nanoclusters for systemic photothermal therapy and efficient renal clearance. Carbohydr Polym. 2020;241:116344.

155. Li H, Wang P, Deng Y, Zeng M, Tang Y, Zhu W-H, et al. Combination of active targeting, enzyme-triggered release and fluorescent dye into gold nanoclusters for endomicroscopy-guided photothermal/photodynamic therapy to pancreatic ductal adenocarcinoma. Biomaterials. 2017;139:30–8.
156. Liu P, Yang W, Shi L, Zhang H, Xu Y, Wang P, et al. Concurrent photothermal therapy and photodynamic therapy for cutaneous squamous cell carcinoma by gold nanoclusters under a single NIR laser irradiation. J Mater Chem B. 2019;7(44):6924–33.
157. Yang Y, Wang S, Wang C, Tian C, Shen Y, Zhu M. Engineered targeted hyaluronic acid–glutathione-stabilized gold nanoclusters/graphene oxide–5-fluorouracil as a smart theranostic platform for stimulus-controlled fluorescence imaging-assisted synergetic chemo/phototherapy. Chem Asian J. 2019;14(9):1418–23.
158. Xie Y, Zheng W, Jiang X. Near-infrared light-activated phototherapy by gold nanoclusters for dispersing biofilms. ACS Appl Mater Interfaces. 2020;12(8):9041–9.
159. Zheng K, Setyawati MI, Leong DT, Xie J. Antimicrobial gold nanoclusters. ACS Nano. 2017;11(7):6904–10.
160. Fang FC. Antimicrobial reactive oxygen and nitrogen species: concepts and controversies. Nat Rev Microbio. 2004;2(10):820–32.
161. Li Y, Qu S, Xue Y, Zhang L, Shang L. Cationic antibacterial metal nanoclusters with traceable capability for fluorescent imaging the nano—bio interactions. Nano Res. 2023;16(1):999–1008.
162. Tao Y, Lin Y, Huang Z, Ren J, Qu X. Incorporating graphene oxide and gold nanoclusters: a synergistic catalyst with surprisingly high peroxidase-like activity over a broad pH range and its application for cancer cell detection. Adv Mater. 2013;25(18):2594–9.
163. Rebilly J-N, Colasson B, Bistri O, Over D, Reinaud O. Biomimetic cavity-based metal complexes. Chem Soc Rev. 2015;44(2):467–89.
164. Wu J, Wang X, Wang Q, Lou Z, Li S, Zhu Y, et al. Nanomaterials with enzyme-like characteristics (nanozymes): next-generation artificial enzymes (II). Chem Soc Rev. 2019;48(4):1004–76.
165. Wang Z, Shao Y, Zhu Z, Wang J, Gao X, Xie J, et al. Novel gold nanozyme regulation strategies facilitate analytes detection. Coord Chem Rev. 2023;495:215369.
166. Wang X-X, Wu Q, Shan Z, Huang Q-M. BSA-stabilized Au clusters as peroxidase mimetics for use in xanthine detection. Biosens Bioelectron. 2011;26(8):3614–9.
167. Wei H, Wang E. Nanomaterials with enzyme-like characteristics (nanozymes): next-generation artificial enzymes. Chem Soc Rev. 2013;42(14):6060–93.
168. Hu D, Sheng Z, Fang S, Wang Y, Gao D, Zhang P, et al. Folate receptor-targeting gold nanoclusters as fluorescence enzyme mimetic nanoprobes for tumor molecular colocalization diagnosis. Theranostics. 2014;4(2):142.
169. Tao Y, Li M, Kim B, Auguste DT. Incorporating gold nanoclusters and target-directed liposomes as a synergistic amplified colorimetric sensor for HER2-positive breast cancer cell detection. Theranostics. 2017;7(4):899.
170. Wang G-L, Jin L-Y, Dong Y-M, Wu X-M, Li Z-J. Intrinsic enzyme mimicking activity of gold nanoclusters upon visible light triggering and its application for colorimetric trypsin detection. Biosens Bioelectron. 2015;64:523–9.
171. Liang M, Yan X. Nanozymes: from new concepts, mechanisms, and standards to applications. Acc Chem Res. 2019;52(8):2190–200.
172. Shen X, Wang Z, Gao XJ, Gao X. Reaction mechanisms and kinetics of nanozymes: insights from theory and computation. Adv Mater. 2024;36(10):2211151. https://doi.org/10.1002/adma.202211151
173. Shen X, Liu W, Gao X, Lu Z, Wu X, Gao X. Mechanisms of oxidase and superoxide dismutation-like activities of gold, silver, platinum, and palladium, and their alloys: a general way to the activation of molecular oxygen. J Am Chem Soc. 2015;137(50):15882–91.
174. Wang Z, Wu J, Zheng J-J, Shen X, Yan L, Wei H, et al. Accelerated discovery of superoxide-dismutase nanozymes via high-throughput computational screening. Nat Commun. 2021;12(1):6866.
175. Mi W, Tang S, Guo S, Li H, Shao N. In situ synthesis of red fluorescent gold nanoclusters with enzyme-like activity for oxidative stress amplification in chemodynamic therapy. Chin Chem Lett. 2022;33(3):1331–6.
176. Deshmukh AR, Aloui H, Kim BS. Novel biogenic gold nanoparticles catalyzing multienzyme cascade reaction: Glucose oxidase and peroxidase mimicking activity. Chem Eng J. 2021;421:127859.
177. Xu D, Wu L, Yao H, Zhao L. Catalase-like nanozymes: classification, catalytic mechanisms, and their applications. Small. 2022;18(37):2203400.
178. Liu CP, Wu TH, Lin YL, Liu CY, Wang S, Lin SY. Tailoring enzyme-like activities of gold nanoclusters by polymeric tertiary amines for protecting neurons against oxidative stress. Small. 2016;12(30):4127–35.
179. Gao L, Liu M, Ma G, Wang Y, Zhao L, Yuan Q, et al. Peptide-conjugated gold nanoprobe: intrinsic nanozyme-linked immunsorbant assay of integrin expression level on cell membrane. ACS Nano. 2015;9(11):10979–90.
180. Lin Y, Ren J, Qu X. Nano-gold as artificial enzymes: hidden talents. Adv Mater. 2014;26(25):4200–17.
181. Mikolajczak DJ, Koksch B. Peptide-gold nanoparticle conjugates as sequential cascade catalysts. ChemCatChem. 2018;10(19):4324–8.
182. Zhang Y, Sun S, Liu H, Ren Q, Hao W, Xin Q, et al. Catalytically active gold clusters with atomic precision for noninvasive early intervention of neurotrauma. J Nanobiotechnol. 2021;19:1–13.
183. Xu Z, Wang T, Li Y, Wen M, Liang K, Ruan C, et al. Nanozyme-engineered bioglass through supercharged interface for enhanced anti-infection and fibroblast regulation. Adv Funct Mater. 2023;33(2):2209438.
184. Shang L, Xu J, Nienhaus GU. Recent advances in synthesizing metal nanocluster-based nanocomposites for application in sensing, imaging and catalysis. Nano Today. 2019;28:100767.
185. Goswami N, Yao Q, Luo Z, Li J, Chen T, Xie J. Luminescent metal nanoclusters with aggregation-induced emission. J Phys Chem Lett. 2016;7(6):962–75.
186. Aires A, Sousaraei A, Moller M, Cabanillas-Gonzalez J, Cortajarena AL. Boosting the photoluminescent properties of protein-stabilized gold nanoclusters through protein engineering. Nano Lett. 2021;21(21):9347–53.
187. Deng H, Huang K, Xiu L, Sun W, Yao Q, Fang X, et al. Bis-Schiff base linkage-triggered highly bright luminescence of gold nanoclusters in aqueous solution at the single-cluster level. Nat Commun. 2022;13(1):3381.